Journal of Hydrology X 1 (2018) 100007

Contents lists available at ScienceDirect

Journal of Hydrology X

journal homepage: www.elsevier.com/locate/hydrolx

Research papers

Application of high-resolution telemetered sensor technology to develop conceptual models of catchment hydrogeological processes

Richard J. Cooper [a,*], Kevin M. Hiscock [a], Andrew A. Lovett [a], Stephen J. Dugdale [a], Gisela Sünnenberg [a], Nicholas L. Garrard [a], Faye N. Outram [a], Zanist Q. Hama-Aziz [b], Lister Noble [c], Melinda A. Lewis [d]

[a] School of Environmental Sciences, University of East Anglia, Norwich Research Park NR4 7TJ, UK
[b] Charmo University, 46023 Chamchamal-Sulaimani, Kurdistan Regional, Iraq
[c] Farm Systems & Environment, Low Road, Wortwell, Harleston IP20 0HJ, UK
[d] British Geological Survey, Wallingford OX10 8BB, UK

ARTICLE INFO

Article history:
Received 30 July 2018
Revised 8 October 2018
Accepted 22 November 2018
Available online 27 November 2018

Keywords:
River
Agriculture
Soil moisture
Groundwater
Surface water
Water pollution

ABSTRACT

Mitigating agricultural water pollution requires changes in land management practices and the implementation of on-farm measures to tackle the principal reasons for water quality failure. However, a paucity of robust empirical evidence on the hydrological functioning of river catchments can be a major constraint on the design of effective pollution mitigation strategies at the catchment-scale. In this regard, in 2010 the UK government established the Demonstration Test Catchment (DTC) initiative to evaluate the extent to which on-farm mitigation measures can cost-effectively reduce the impacts of agricultural water pollution on river ecology while maintaining food production capacity. A central component of the DTC platform has been the establishment of a comprehensive network of automated, web-based sensor technologies to generate high-temporal resolution empirical datasets of surface water, soil water, groundwater and meteorological parameters. In this paper, we demonstrate how this high-resolution telemetry can be used to improve our understanding of hydrological functioning and the dynamics of pollutant mobilisation and transport under a range of hydrometerological and hydrogeological conditions. Furthermore, we demonstrate how these data can be used to develop conceptual models of catchment hydrogeological processes and consider the implications of variable hydrological functioning on the performance of land management changes aimed at reducing agricultural water pollution.

1. Introduction

Diffuse pollution from agriculture is a major driver behind the degradation of freshwater systems, causing an array of detrimental economic (Färe et al., 2006; Popp et al., 2012; Pretty et al., 2003) and environmental (Hilton et al., 2006; Skinner et al., 1997; Smith et al., 1999) impacts that threaten the ability of these systems to provide ecosystem services (Némery and Garnier, 2016; Quinton et al., 2010). In the European Union, the response to this issue has been to implement the Water Framework Directive (WFD; 2000/60/EC) which requires member states to achieve good qualitative and quantitative status of all surface, subsurface and marine waterbodies up to 1 nautical mile offshore. These waterbodies are divided into River Basin Districts (RBDs) based on river catchment area. National governments within each RBD are required to produce a holistic river basin management plan to provide a clear strategy and timeframe for how the status of waterbodies within the RBD will be improved from source to mouth (Hering et al., 2010; Voulvoulis et al., 2017).

Achieving reductions in agricultural pollution within RBDs requires changes in land management and the implementation of mitigation measures to tackle the principal reasons for water quality failure. However, a paucity of robust empirical evidence on the hydrological functioning of individual river catchments, particularly in relation to the dynamics of pollutant mobilisation and transport under a range of hydrometerological and hydrogeological conditions, can be a major constraint on the design of effective pollution mitigation strategies at the catchment-scale (Allen et al., 2014; Harvey and Gooseff, 2015; Rode et al., 2016). For example, the porosity and permeability of catchment bedrock affects aquifer storage properties and the support of river baseflow (Cook, 2015); the type, thickness and hydraulic conductivity of superficial geological deposits affects shallow groundwater movement and the transport of leached pollutants (Nolan and Hitt, 2006); the composition of the hyporheic zone determines groundwater-surface

* Corresponding author.
E-mail address: Richard.J.Cooper@uea.ac.uk (R.J. Cooper).

https://doi.org/10.1016/j.hydroa.2018.100007
2589-9155/

water interactions and the movement and storage of pollutants across and within the riverbed (Gomez-Velez and Harvey, 2014; Rode et al., 2015; Newcomer et al., 2018); river channel morphology, sinuosity, gradient, stream order and connectivity impact upon hydrological functioning and the speed of pollutant transport (Garnier et al., 2002); within-channel processes such as the growth of macrophytes and bacterial communities impact upon the interception, utilisation and consumption of nutrients (Withers and Jarvie, 2008); whilst the climate regime controls the temporal dynamics (i.e. flushing) of dissolved and particulate pollutants through catchments (Halliday et al., 2012; Halliday et al., 2014).

Of particular interest here the hydrogeology of catchments affects both pollutant mobility within the environment and its delivery pathway from source to receptor and this consequently affects within-river pollutant behaviour (Dupas et al., 2015; Dupas et al., 2016). It is especially important to understand how the hydrogeology of a catchment impacts upon pollutant travel times, which can range from minutes for rapid surface flow paths to decades for slower subsurface routes (Bowes et al., 2015; King et al., 2015). Constructing a detailed understanding of pollutant transport is essential when it comes to assessing the effectiveness of targeted pollutant mitigation measures, as judgements made without the context of pollutant travel times could result in measures incorrectly being assessed as a success or failure before sufficient time has passed for the pollutant to reach the receptor (Allen et al., 2014).

Established in 2010, the Demonstration Test Catchment (DTC) platform is a UK government initiative funded by the Department for Environment, Food and Rural Affairs (Defra) working in four English catchments to evaluate the extent to which on-farm mitigation measures can cost-effectively reduce the impacts of agricultural water pollution on river ecology while maintaining food production capacity (McGonigle et al., 2014). Each DTC focuses on a different type of farming system, namely, intensive arable (River Wensum DTC, Norfolk), upland livestock (River Eden DTC, Cumbria) and mixed farming (River Avon DTC, Hampshire; River Tamar DTC, Devon/Cornwall). Research outputs from the DTCs have included assessments of the effectiveness of a biobed (Cooper et al., 2016a), cover crops and non-inversion tillage (Cooper et al., 2017), farm track resurfacing (Biddulph et al., 2017) and constructed wetlands (Cooper et al., 2019) as mitigation measures for reducing agricultural pollution. Research has also explored the factors controlling nutrient transfers to agricultural headwater streams (Lloyd et al., 2016a; Lloyd et al., 2016b; Outram et al., 2016; Perks et al., 2015), hydrochemical responses of rivers to extreme weather events (Cooper et al., 2015c; Ockenden et al., 2017; Outram et al., 2014), the impacts of invasive species on water quality (Cooper et al., 2016b) and the apportionment of sources of fluvial sediments to soils eroding under different land uses (Collins et al., 2013; Cooper et al., 2015a; Cooper et al., 2015b).

A central component of the DTC platform underlying this previous research has been the establishment of a comprehensive network of automated web-based sensor technologies to generate high-temporal resolution empirical datasets of surface water, soil water, groundwater and meteorological parameters. Whilst numerous catchment-scale environmental research programmes (e.g. Critical Zone Observatories) have been established across Europe (Garnier and Billen, 2016; Vuorenmaa et al., 2018) and the United States (Brantley et al., 2017; Kim et al., 2017) in recent years, only a few have managed to produce comprehensive datasets of environmental variables at the 15–30 min resolution of the DTC platform over timescales of >5 years. The near unprecedented level of detail generated by such an intensive monitoring network means the DTCs are uniquely placed to deliver advancements in our understanding of hydrological functioning at the catchment-scale (Covino, 2017).

Focusing on the River Wensum DTC, the aim of this paper is to demonstrate how such high-resolution data can be used to improve our understanding of hydrological functioning and pollutant pathways and, in turn, how this can be used to develop conceptual models of catchment hydrogeological processes (e.g. Harvey and Gooseff, 2015; Rode et al., 2016). This paper:

(i) presents the experimental design of the River Wensum DTC for generating high-resolution datasets of river water, groundwater, soil water and meteorological parameters;
(ii) contrasts the temporal and spatial dynamics of these hydrological parameters in areas with contrasting geology and soil type over six hydrological years (2011–2017);
(iii) develops conceptual models of catchment hydrogeological processes informed by high-resolution empirical datasets;
(iv) considers the implications of hydrogeological characteristics for the implementation of on-farm mitigation measures to reduce agricultural pollution

2. Material and methods

2.1. River Wensum

The River Wensum, Norfolk, is a 78 km length lowland, calcareous, river that rises near the village of South Raynham (52°46′N, 0°47′E) ~75 m above sea level and flows southeast before merging with the River Yare south of Norwich (52°37′16″ N, 1°19′22″ E) (Fig. 1). In total, it drains an area of 660 km^2 and has a mean annual discharge of 4.1 m^3 s^{-1} near its outlet (CEH, 2017) and annual baseflow indices (BFI) ranging from 0.5 to 0.9. In 1993, a 71 km stretch of the Wensum from South Raynham to Hellesdon Mill, Norwich, was designated a whole-river Site of Special Scientific Interest (SSSI) in recognition of it being one of the best examples of a lowland calcareous river system in the UK (Sear et al., 2006). In 2001, the Wensum was given further European Special Area of Conservation (SAC) status due to the diversity of its internationally important flora and invertebrate fauna. However, the ecological condition of the Wensum is in decline, with 99.4% of the protected habitat considered to be in an unfavourable or declining state due, primarily, to excessive sediment and nutrient loadings from agriculture and sewage treatment works (Grieve et al., 2002; Sear et al., 2006). Arable agriculture dominates land use across the catchment (63%) and it is due to the impact of agriculture on water quality that the River Wensum was chosen as one of four DTC study catchments by the UK government.

2.2. Blackwater Drain sub-catchment

The Wensum catchment comprises 20 sub-catchments, one of which, the 19.7 km^2 Blackwater Drain, represents the area intensively studied as part of the River Wensum DTC and provides the focus of this paper. For monitoring purposes, the Blackwater Drain is further divided into six mini-catchments named *A* to *F*, across which there is a pronounced contrast in the superficial geology and soil type (Fig. 1). The western section (mini-catchments A + B) is underlain by a complex sequence of Mid-Pleistocene chalky, flint-rich, argillaceous glacial tills of the Sheringham Cliffs (Bacton Green Till Member; 0.2–7 m depth) and Lowestoft (Lowestoft Till Member; 8–16 m depth) Formations, with interdigitated bands of glaciofluvial and glaciolacustrine sands and gravels (Table 1; Fig. 2). In turn, these are superimposed onto the quartzite-rich marine sands and gravels of the Lower Pleistocene Wroxham Crag Formation (16–22 m depth), which overlies the Cretaceous Chalk

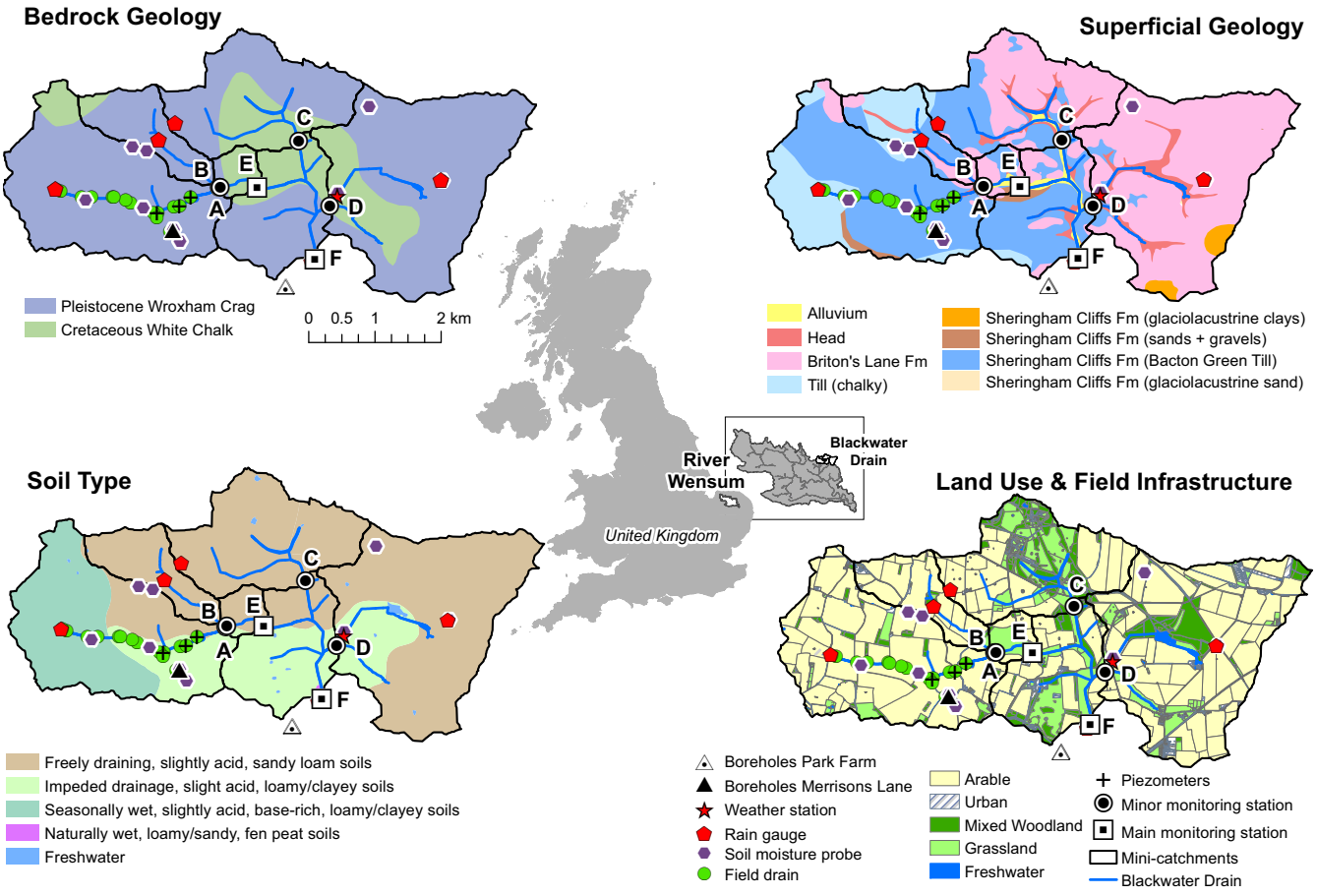

Fig. 1. Spatial variability in bedrock geology (BGS; 1:10,000), superficial geology (BGS; 1:10,000), land use (LCM2007) and soil type (LandIS) across the Blackwater Drain sub-catchment of the River Wensum, UK. Also showing the layout of field monitoring infrastructure and mini-catchment boundaries. Geological maps reproduced with the permission of the British Geological Survey, ©NERC; LCM2007© and database right NERC (CEH) 2011 (Morton et al., 2011). All rights reserved. Contains Ordnance Survey data © Crown copyright and database right 2007. © third party licensors.

Table 1
Hydrogeological succession of the Blackwater Drain sub-catchment.

System	Series	Formation	Member	Lithology	Approx. thickness (m)	Hydrogeological type
Quaternary	Holocene	Recent deposits	–	Head, alluvium, river terrace deposits	0–3	Minor aquifer
	Mid-Pleistocene (MIS 12)	Briton's Lane	–	Undifferentiated, glaciofluvial outwash sands and gravels	0–7	Minor aquifer
		Sheringham Cliffs	Bacton Green Till;	Undifferentiated, glacigenic chalk-rich, clays and sands;	0–10;	Aquitard;
			Sands + gravels	Glaciofluvial + glaciolacustrine sands and gravels	0–10 (patchy)	Minor aquifer
		Lowestoft	Lowestoft Till	Undifferentiated, glacigenic, argillaceous matrix with abundant chalk and flint clasts	0–10	Aquitard
		Happisburgh	Sands + gravels; Happisburgh Till	Glaciofluvial + glaciolacustrine sands and gravels; Undifferentiated, sandy grey matrix with flint and chalk clasts	0–5; 0–2	Minor aquifer
	Lower Pleistocene	Wroxham Crag	–	Marine, quartzite and flint-rich sands and gravels	0–5	Minor aquifer
Cretaceous	Upper Cretaceous	White Chalk Subgroup	–	Fine-grained fissured limestone with flints	350	Major aquifer

(>22 m depth). The Chalk, which has a mean storage coefficient of 0.064, transmissivity of 685 m^2 d^{-1} and effective fracture porosity of 1–2%, serves as the principal aquifer for this region, supplying ~40% of public water supply in East Anglia and up to 90% in some rural areas of north Norfolk (Hiscock et al., 2001; Toynton, 1983). Within the river valley, Holocene-age alluvium and river terrace deposits overlie this sequence (Hiscock et al., 1996). The soils in this western section are predominantly clay loams of the argillic brown earths (Freckenham series) and stagnogley (Beccles series) groups which, together with the argillaceous tills, result in moderately impeded drainage conditions in the western section of the sub-catchment.

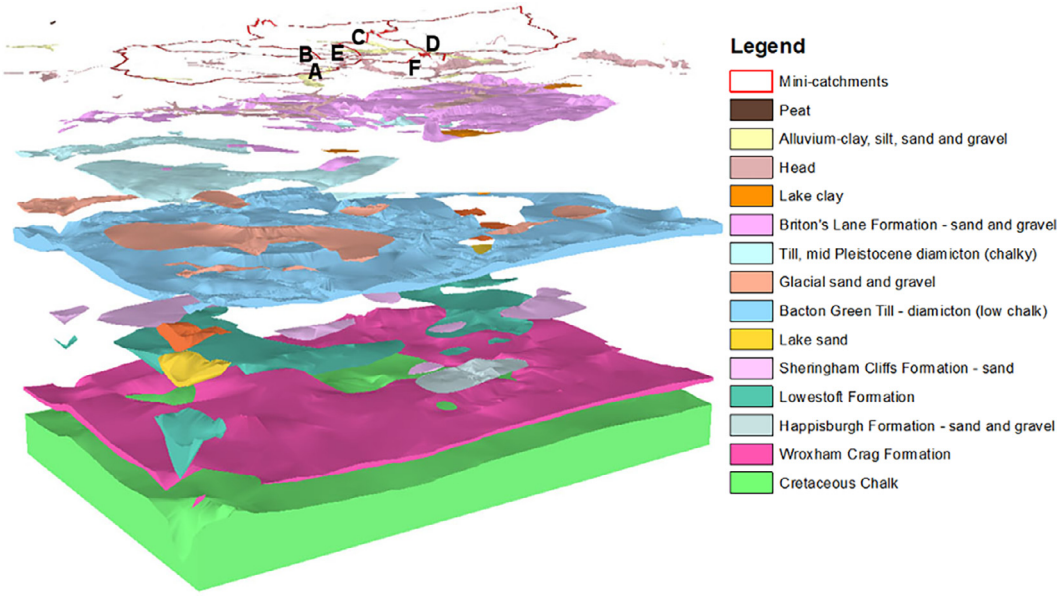

Fig. 2. An expanded 3-D geological model of the Blackwater Drain sub-catchment, Norfolk, UK. Letters refer to the locations of the bankside monitoring stations. BGS © UKRI 2018.

In contrast, the eastern section (mini-catchments C + D) is more freely draining with sheets of glacial outwash sands and gravels of the Mid-Pleistocene Briton's Lane Formation (0.2–7 m depth) overlying the clay-rich Bacton Green Till Member (6–10 m depth) (Table 1; Fig. 2). As with the western section, the Sheringham Cliffs Formation tills contain interdigitated higher permeability, glaciolacustrine sands (8–10 m). Underlying this is a comparatively thin layer of chalky, argillaceous till of the Lowestoft Formation (10–12 m depth), which in turn overlies glaciofluvial, glaciolacustrine and glaciogenic sands, gravels and tills of the Happisburgh Formation (12–17 m depth). Lastly, as in the western section, the Wroxham Crag Formation (17–22 m depth) overlies Cretaceous Chalk (>22 m depth) (Lewis, 2014). The soils in the eastern section are predominately freely draining, sandy loams of the brown sands (Hall series) and brown earth (Sheringham series) groups.

Topographically, the Blackwater Drain sub-catchment is ideally suited to arable farming, being 30–50 m above sea level and having gentle slopes that rarely exceed 0.5° of inclination. As such, land use is dominated by intensive arable cultivation, ranging from 60% on the lower fertility sandy loam soils of mini-catchment C, to 92% on the fertile clay loam soils of mini-catchment A. Winter wheat, winter and spring barley, sugar beet, oilseed rape and spring beans are the dominant crop types, with these being grown in a seven-year rotation across much of the western half of the sub-catchment. The remainder of the land use is comprised of improved grassland (12%), rough grassland (2%), mixed woodland (11%), freshwater (<1%) and rural settlements (1%).

2.3. Experimental design

2.3.1. Meteorological monitoring

Meteorological data at 15-min resolution are generated from two weather stations installed at sites A and D (Fig. 1). These record precipitation via tipping-bucking rain gauges, alongside measurements of temperature, wind speed, humidity and net solar radiation. In addition, five further tipping bucket rain gauges distributed across the sub-catchment also record precipitation at 15-min intervals and these data are compiled into a single master record based on the median of the five records. All weather station data are uploaded to web-based servers in near real-time via wireless telemetry (Meteor Communications Ltd.; Isodaq Technology). Precipitation and temperature records are compared against the UK Met Office 1981–2010 monthly averages for this area based on a weather station at Coltishall, Norfolk (Met Office, 2017).

2.3.2. Riverine monitoring

At the outlet of the six Blackwater Drain mini-catchments (A – F), a bankside monitoring station makes semi-continuous measurements of river water quality parameters at 30-min resolution (Figs. 1 and 3 & S4–S8). All monitoring stations measure temperature, conductivity, pH, turbidity, dissolved oxygen and ammonium via multi-parameter sondes (YSI 6600) mounted in flow-through cells. In addition, two larger monitoring stations at sites E and F measure nitrate-N (Hach Lange Nitratax SC optical probe), total phosphorus (TP) and total reactive phosphorus (TRP) (Hach Lange Sigmatax SC combined with Phosphax Sigma). River stage is measured using pressure transducers housed in stilling wells (Impress IMSL Submersible Level Transmitter) and this is converted into river discharge via stage-discharge rating curves constructed from manual flow gauging with an open-channel EM flow meter (Figs. S2 and S3). Discharge values are presented within 95% confidence intervals generated from the non-linear least-squares regression rating curve (Outram et al., 2014; 2016). As with the meteorological data, all data are uploaded to a web-based server in near real-time via wireless telemetry (Meteor Communications Ltd.).

2.3.3. Groundwater monitoring

Groundwater data are generated from two sets of boreholes which capture the influence of the different geologies between the eastern and western parts of the catchment. The western set of boreholes (Merrisons Lane MLBH1–4; 52°46′54″ N, 1°07′05″ E) are drilled to depths of 50 m (Chalk), 15 m (Lowestoft Formation), 12 m (Sheringham Cliffs Formation – sands and gravels) and 4 m (Sheringham Cliffs Formation – Bacton Green Till Member). The eastern set (Park Farm PFBH1–4; 52°46′25″ N, 1°08′33″ E) are drilled to depths of 48 m (Chalk), 17 m (Happisburgh Formation – sands and gravels), 10 m (Sheringham Cliffs Formation – sands and gravels) and 6 m (Britons Lane Formation). Each borehole is equipped with a pressure transducer (Mini-Diver, Schlumberger)

Fig. 3. Photographs of the River Wensum DTC study sites. Clockwise from top left: mini-catchment A (channel width ~2 m); site F (channel width ~4 m); mini-catchment C (channel width ~2 m); and a telemetered bankside monitoring station at site C.

which records temperature and pressure at 15-min resolution and is manually downloaded every 2–3 months and barometrically compensated by linear interpolation using the barometer located at each borehole set (BARO, Schlumberger).

2.3.4. Hyporheic zone monitoring

To provide an insight into catchment hydrological connectivity, groundwater-surface water interactions within the hyporheic zone were monitored via a network of 15 piezometers installed across five locations along a 1.6 km reach of the Blackwater Drain upstream of monitoring site E (Fig. 1). At each site, three drive-tip, galvanised steel piezometers with a screened tip section containing a filter membrane (Marton Geotechnical Services LTD) were installed to depths of 0.5, 1.0 and 1.5 m beneath the riverbed. At approximately monthly intervals between April 2016 and January 2017, the piezometers were evacuated using a hand siphon pump before being allowed to refill over a period of ~3 h. Following incubation, piezometer water column heights were measured to calculate infiltration rates and estimate the hydraulic conductivity of the subsurface sediments beneath the riverbed. Sediment coring was also undertaken at all piezometer sampling sites at the 0.5 m and 1.0 m depths to facilitate particle size analysis and measurements of bulk density and porosity to determine the nature of the hyporheic zone deposits.

2.3.5. Soil water monitoring

Soil moisture content data are generated at 15-min resolution through 10 capacitance-based soil moisture probes installed across the mini-catchments (Fig. 1), which measure percentage water content and temperature at 10 cm intervals at 10–90 cm depth. Wireless telemetry is used to upload the data in near real-time to a web server for utilisation (ADCON Telemetry). Furthermore, most of the arable land in the western Blackwater catchment on clay-rich soils is extensively under-drained by a dense network of plastic and concrete agricultural field drains installed in a herringbone layout at depths of 1.0–1.5 m during numerous phases of land drainage over past decades. Across mini-catchment A, 143 drains were identified discharging soil water directly into the river at a density of 43 outflows per km. A further 18 drain outflows were identified in mini-catchment B at a density of 16 per km. Grab samples (1 l) of this soil water were collected from a subset of 17 drains in mini-catchment A at approximately weekly intervals and the drain flow rate (L s^{-1}) recorded at the time of sampling. Of these 17 drains, 14 underdrain clay and clay loam soils, while just three underdrain sandy loam soils reflecting the reduced requirement for artificial drainage under higher permeability soils.

2.4. Data analysis

Hydrograph separation was conducted following application of the Boughton two-parameter algorithm approach (Chapman, 1999) to river discharge data in order to derive baseflow discharge (m^3 s^{-1}) for each location. The separation algorithm is as follows:

$$Q_b(i) = \frac{k}{1+C} Q_b(i-240) + \frac{C}{1+C} Q(i)$$

where Q_b is baseflow discharge; k (0.99) and C (0.1) are recession constants; i is the time-step; and 240 represents the 5 day integration period over which baseflow is calculated (i.e. 30 min data × 5 days = 240 half hour measurements). The baseflow index (BFI) was subsequently calculated as the ratio of baseflow discharge to total discharge. Annual rainfall runoff coefficients were calculated as the ratio of total discharge volume across the catchment area (mm) to annual precipitation totals (mm).

A catchment water balance equation was used to calculate evapotranspiration, E_T, as follows:

$$E_T = P - S_R - G_R \pm \Delta S$$

where P is precipitation; S_R is surface water runoff; G_R is groundwater discharge; and ΔS is the change in soil and groundwater storage. Groundwater storage coefficients (S) were calculated as follows:

$$S = \frac{G_R}{\Delta h}$$

where Δh is the amplitude of annual groundwater level change in the shallow borehole (i.e. MLBH4; PFBH4).

3. Results and discussion

3.1. Meteorological parameters

Annually, precipitation totals varied from a low of 632 mm during the 2016/17 hydrological year (October – September), 6% below the 1981–2010 average for this area (674 mm; (Met Office, 2017), to a high of 742 mm during the 2015/16 hydrological year, 10% above average (Table 2). July 2013 (11 mm) and May 2014 (120 mm) were the driest and wettest months, respectively, with these receiving 20% and 253% of the average monthly precipitation (Fig. 4). The highest recorded rainfall intensity was 60 mm h^{-1} observed during a heavy thunderstorm on the 20th June 2015. The longest near continuous period of wet conditions was between March 2012 and March 2013 when 11 of out 13 months recorded above average precipitation. This was immediately followed by the longest period of dry conditions between April and September 2013 when five out of six months recorded below average rainfall. However, the most significant winter recharge period deficit occurred from October 2011 – February 2012 when precipitation totals were 40% below average. In this period, just 33% of total annual rainfall in 2011/12 fell during the important October – March recharge season, compared with an average of 55% during the following five hydrological years.

With respect to temperature, the monitoring period started off relatively cold with temperatures below average for 19 out of 22 months between February 2012 and November 2013, with the mean temperature for this period 1.3 °C below the 1981–2010 average (10.2 °C) (Fig. 5). This was followed by 16 months of near average temperatures before a sustained warm period from April 2015 to June 2017 recorded 23 out of 27 months with above average temperatures. The mean temperature during this warm period was 1.2 °C above the long-term average. December 2015 was the warmest month relative to average with monthly mean temperatures 6.7 °C higher, whilst March 2013 was the coldest month relative to average with temperatures 4.3 °C lower. The highest maximum recorded temperature was 32.8 °C on the 1st July 2015, with the lowest minimum temperature of −16.6 °C recorded on the 16th January 2013.

3.2. Surface hydrology

Total annual river discharge volumes at the outlet of mini-catchment A (5.4 km^2), which drains the lower permeability Bacton Green Till Member deposits, ranged from 5.09×10^5 m^3 a^{-1}

Table 2
Annual hydrological summaries for sites A, C and F for the hydrological years 2011/12 to 2016/17. Numbers in parentheses represent one standard deviation.

Parameter	Type	2011/12	2012/13	2013/14	2014/15	2015/16	2016/17
Meteorology	Mean total rainfall (mm)	694	638	724	715	742	632
	Mean air temperature (°C)	9.7	8.6	10.0	10.2	12.3	10.2
	Mean net solar radiation (W m^{-2})	40.6	42.2	38.5	41.3	41.5	45.3
Surface Hydrology	Total discharge volume (m^3 a^{-1})	$6.97 \times 10^{5*}$	9.64×10^5	6.95×10^5	8.46×10^5	7.16×10^5	5.09×10^5
	Total discharge volume (mm)	130*	180	129	158	133	95
Site A	Annual rainfall runoff coefficient	0.19	0.28	0.18	0.22	0.18	0.15
5.4 km^2	Baseflow volume (m^3)	3.22×10^5	4.54×10^5	3.99×10^5	4.73×10^5	3.39×10^5	2.64×10^5
	Baseflow volume (mm)	60	85	74	88	63	49
	Baseflow index (BFI)	0.46	0.47	0.57	0.56	0.47	0.52
Surface Hydrology	Total discharge volume (m^3 a^{-1})	$4.35 \times 10^{5*}$	1.13×10^6	9.35×10^5	7.42×10^5	9.75×10^5	1.12×10^6
	Total discharge volume (mm)	124*	321	266	211	278	318
Site C	Annual rainfall runoff coefficient	0.18	0.50	0.37	0.30	0.37	0.50
3.5 km^2	Baseflow volume (m^3)	3.22×10^5	8.35×10^5	7.40×10^5	6.01×10^5	7.60×10^5	9.23×10^5
	Baseflow volume (mm)	92	237	210	171	216	262
	Baseflow index (BFI)	0.74	0.74	0.79	0.81	0.78	0.82
Surface Hydrology	Total discharge volume (m^3 a^{-1})	2.14×10^6	3.94×10^6	3.02×10^6	2.27×10^6	3.84×10^6	2.55×10^6
	Total discharge volume (mm)	109	200	153	115	195	129
Site F	Annual rainfall runoff coefficient	0.16	0.31	0.21	0.16	0.26	0.20
19.7 km^2	Baseflow volume (m^3)	1.39×10^6	2.52×10^6	1.99×10^6	1.55×10^6	2.46×10^6	1.78×10^6
	Baseflow volume (mm)	71	128	101	79	125	90
	Baseflow index (BFI)	0.65	0.64	0.66	0.68	0.64	0.70
Groundwater	Mean level in borehole ML1 (m asl)	39.5 (0.3)	40.4 (0.5)	40.1 (0.3)	39.8 (0.4)	40.3 (0.5)	40.0 (0.4)
Merrisons Lane	Mean level in borehole ML2 (m asl)	39.8 (0.4)	41.3 (0.5)	40.8 (0.4)	40.6 (0.6)	40.7 (0.5)	40.7 (0.6)
	Mean level in borehole ML3 (m asl)	40.3 (0.6)	41.2 (0.5)	40.8 (0.4)	41.0 (0.3)	41.5 (0.3)	40.9 (0.6)
	Mean level in borehole ML4 (m asl)	41.1 (0.9)	41.7 (0.5)	41.5 (0.5)	41.2 (0.7)	41.5 (0.6)	41.1 (0.8)
Groundwater	Mean level in borehole PF1 (m asl)	31.2 (0.2)	31.8 (0.3)	31.6 (0.2)	31.5 (0.2)	31.7 (0.3)	31.6 (0.1)
Park Farm	Mean level in borehole PF2 (m asl)	31.4 (0.2)	32.1 (0.4)	31.8 (0.2)	31.7 (0.2)	32.0 (0.3)	31.7 (0.2)
	Mean level in borehole PF3 (m asl)	32.4 (0.3)	33.2 (0.4)	33.1 (0.2)	32.7 (0.2)	33.0 (0.4)	32.8 (0.1)
	Mean level in borehole PF4 (m asl)	33.4 (0.3)	34.0 (0.3)	33.8 (0.2)	33.6 (0.1)	33.9 (0.3)	33.7 (0.1)

* Missing data from October & November 2011.

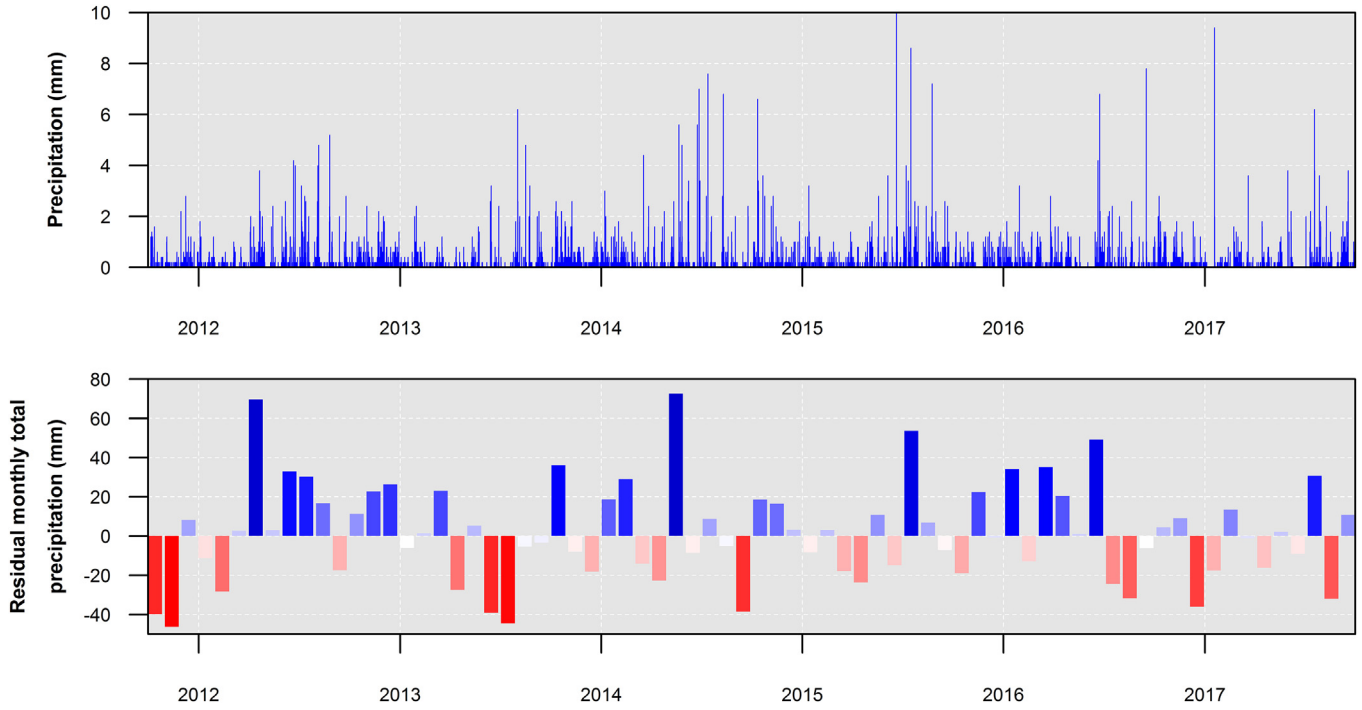

Fig. 4. Precipitation records for weather station A between October 2011 and September 2017 at 15-min resolution (top) and as monthly total residuals from the Met Office 1981–2010 average for Coltishall (bottom).

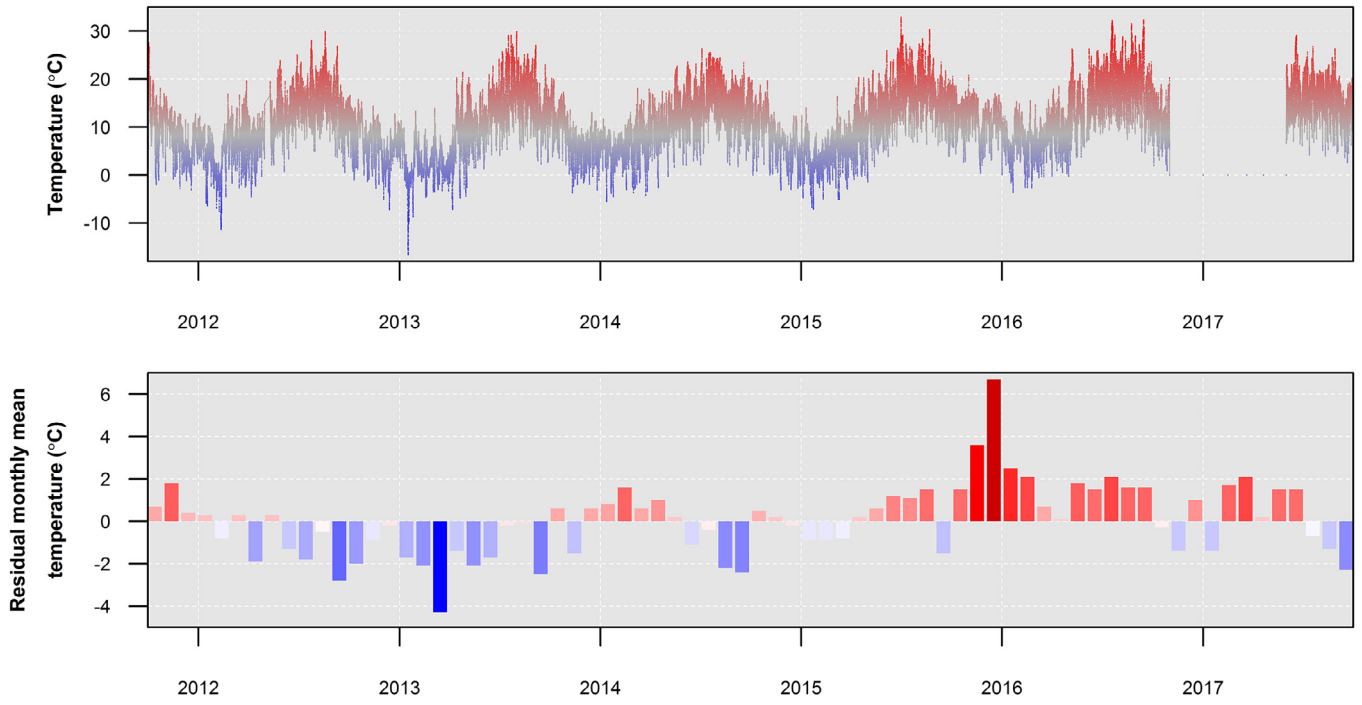

Fig. 5. Air temperature records for weather station A between October 2011 and September 2017 at 15-min resolution (top) and as monthly mean residuals from the Met Office 1981–2010 average for Coltishall (bottom). Missing 15-min resolution temperature data caused by instrument failure; substituted with data from a nearby station for monthly residuals.

(95 mm) in 2016/17 to 9.64×10^5 m^3 a^{-1} (180 mm) in 2012/13, yielding annual rainfall runoff coefficients from 0.15 to 0.28 (Table 2; Fig. 6). Annual baseflow volumes ranged from 2.64×10^5 m^3 a^{-1} (49 mm) in 2016/17 to 4.73×10^5 m^3 a^{-1} (88 mm) in 2014/15, with baseflow indices of 0.46–0.57. The lowest and highest total discharges recorded were 0.0004 m^3 s^{-1} (May 2013) and 0.572 m^3 s^{-1} (June 2016), respectively, meaning the highest peak discharge was 1430 times greater than the minimum flow.

Conversely, at the outlet to mini-catchment C (3.5 km^2), which drains the higher permeability sands and gravels of the Briton's Lane Formation, mean annual river discharge was 20% higher than

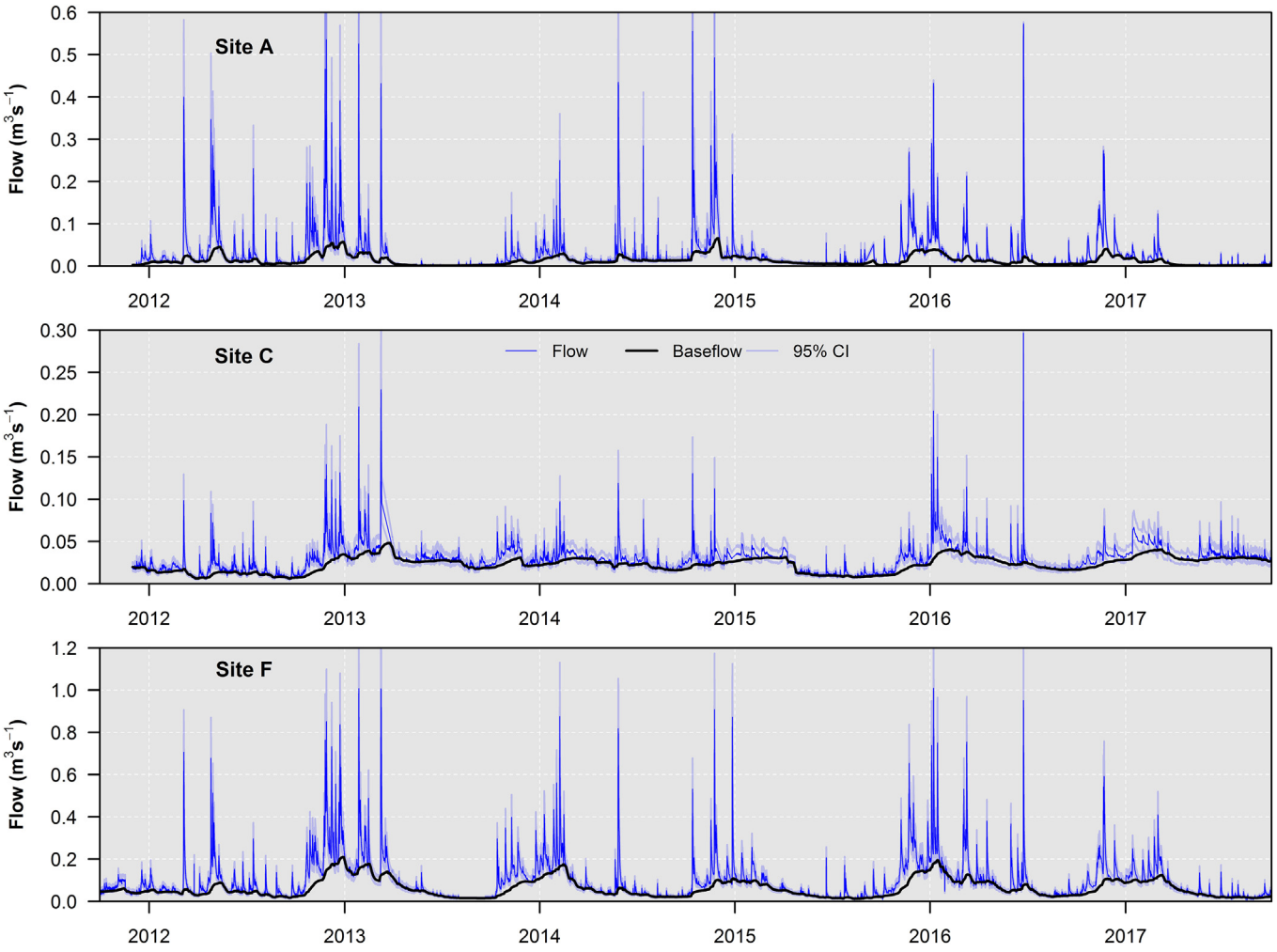

Fig. 6. River flow records (30-min resolution) derived from stage-discharge relationships at three sites in the Blackwater Drain sub-catchment between October 2011 and September 2017. Confidence intervals reflect uncertainty in the rating curves.

recorded at site A, this despite the catchment area being 35% smaller. Total discharge volumes ranged from 7.42×10^5 m^3 a^{-1} (211 mm) in 2014/15 (excluding 2011/12 due to missing data) to 1.13×10^6 m^3 a^{-1} (321 mm) in 2012/13, with annual rainfall runoff coefficients of 0.30–0.50. The lowest and highest total discharges recorded were 0.0049 m^3 s^{-1} (September 2012) and 0.296 m^3 s^{-1} (June 2016), respectively, revealing the maximum peak discharge was just 60 times greater than the minimum recorded flow. This reduced variability in flow range compared to site A reflects a fluvial system with greater baseflow input at site C, with baseflow volumes ranging from 6.01×10^5 m^3 a^{-1} (171 mm) to 9.23×10^5 m^3 a^{-1} (262 mm) and yielding much higher baseflow indices of 0.74–0.82. The permeable sandy glacial deposits within mini-catchment C result in lower surface water runoff during winter due to greater direct recharge to groundwater, and higher flows during the summer due to greater baseflow input to total runoff. This contrasts with mini-catchment A, where river flows are higher during winter due to increased surface water runoff from the less permeable argillaceous glacial deposits, and lower during the summer due to a lower baseflow input to total runoff.

At the Blackwater Drain sub-catchment outlet (site F; 19.7 km^2), total annual river discharge ranged from a low of 2.14×10^6 m^3 a^{-1} in 2011/12 to a high of 3.94×10^6 m^3 a^{-1} in the following hydrological year 2012/13. This equates to a total discharge depth across the whole sub-catchment of 109–200 mm, respectively, and annual rainfall runoff coefficients of 0.16–0.31. The low flows in 2011/12 can be attributed to low precipitation totals during the winter recharge period (Fig. 7) which resulted in total discharge volumes during October – March accounting for just 48% of the annual flow compared to an average of 78% during the following five years. The maximum recorded total discharge (1.009 m^3 s^{-1}) was 136 times greater than the lowest recorded discharge (0.0074 m^3 s^{-1}). Baseflow volumes similarly varied from a low of 1.39×10^6 m^3 a^{-1} (71 mm) in 2011/12 to 2.52×10^6 m^3 a^{-1} (128 mm) in 2012/13, with baseflow indices of 0.64–0.70. These BFI values are intermediate to those observed at sites A and C and reflect the combination of both low permeability Bacton Green Till Member deposits (53% spatial coverage) and high permeability Briton's Lane Formation deposits (47% spatial coverage) across the catchment.

3.3. Groundwater hydrology

Mean annual groundwater levels recorded at both the Merrisons Lane and Park Farm sites (Fig. 8) were lowest at all depths (4–50 m) during 2011/12 and highest during the following hydrological year (2012/13). Additionally, groundwater levels at both sites were always 2.6–7.2 m above the river water level and thus the Blackwater Drain was gaining water from either upwelling through the riverbed or through groundwater discharging into the river at field drain outflows (e.g. Brunner et al., 2011). However, the degree of temporal variability observed in groundwater levels

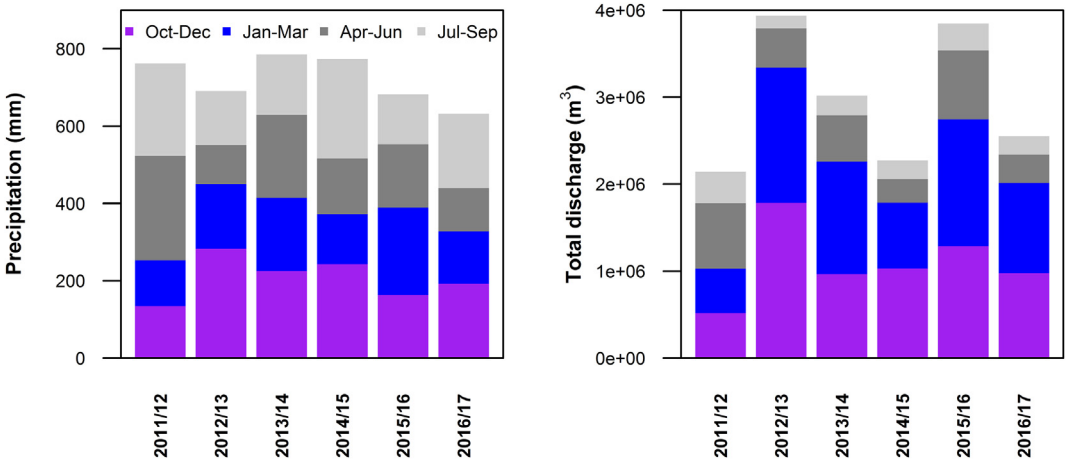

Fig. 7. Stacked bar charts of quarterly precipitation (left) and total discharge at site F (right) for hydrological years 2011/12 to 2016/17.

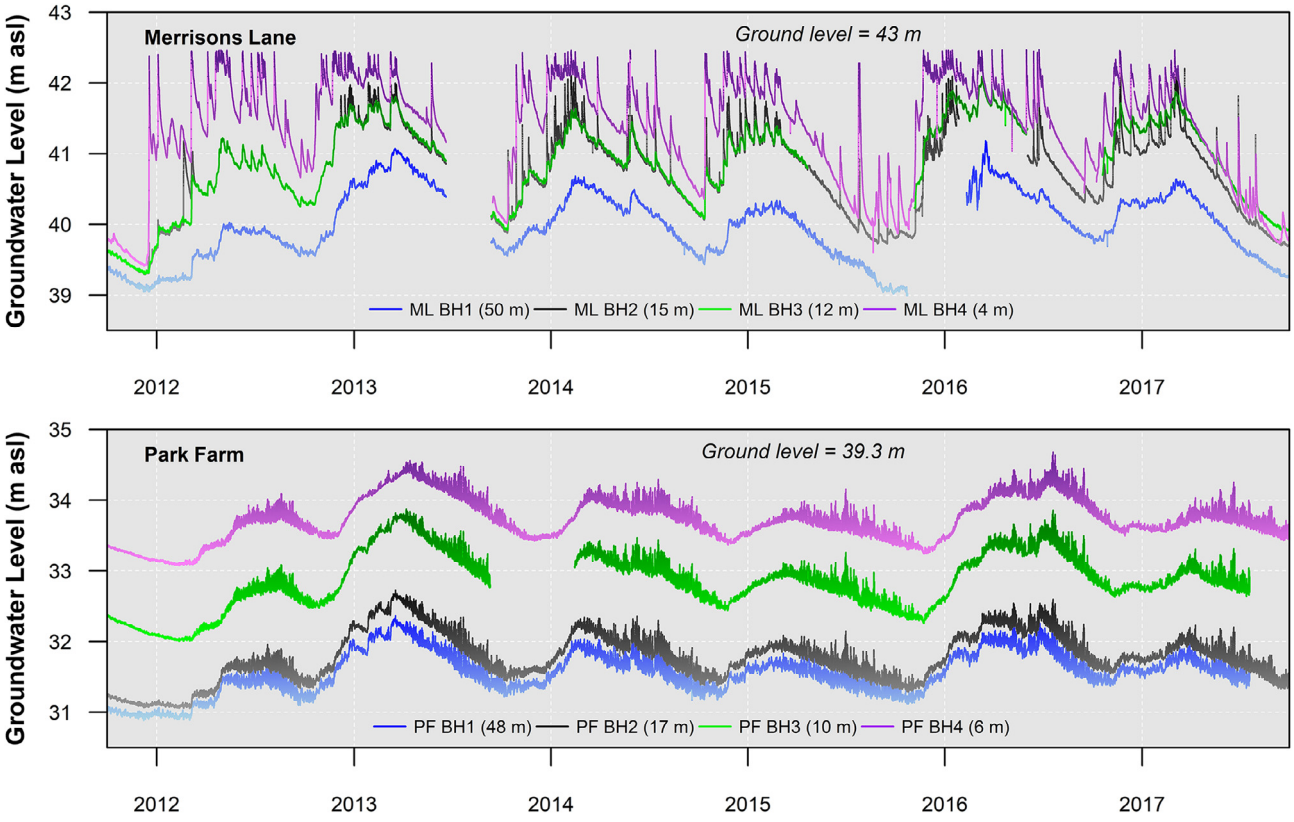

Fig. 8. Groundwater levels recorded (15-min resolution) in boreholes at two locations in the Blackwater Drain sub-catchment between October 2011 and September 2017. Superficial Quaternary geology is dominantly clay-rich glacial till at Merrisons Lane and glaciofluvial/glaciolacustrine sands and gravels at Park Farm.

differed considerably depending upon the superficial Quaternary geology. Beneath the argillaceous, lower permeability glacial deposits at Merrisons Lane there was considerable temporal variability at monthly to annual timescales, with the 50 m depth Chalk borehole recording a 2.20 m range in hydraulic head between the lowest (38.99 m a.s.l.) and highest (41.19 m a.s.l.) values. Similarly, in the shallow (4 m) Bacton Green Till borehole at this site a 3.06 m range in hydraulic head was recorded between the lowest (39.41 m a.s.l.) and highest levels (42.47 m a.s.l.). These values contrast strongly with groundwater levels recorded under the higher permeability sandy deposits at the Park Farm boreholes where a more muted response was observed. At Park Farm, a 1.49 m range in hydraulic head was observed between the lowest (30.88 m a.s.l.) and highest (32.37 m a.s.l.) levels in the 48 m depth Chalk borehole, whilst a 1.60 m head range was recorded in the 6 m depth Briton's Lane Formation borehole between the lowest (33.08 m a.s.l.) and highest (34.68 m a.s.l.) recorded levels.

These observations reflect the lower storage coefficient of the argillaceous Bacton Green Till Member and Lowestoft Formation at Merrisons Lane (see Section 3.6) which make groundwater levels here more responsive to antecedent conditions (i.e. wetting and drying) at monthly to annual timescales as there is a smaller volume of effective water stored within these superficial deposits (Allen et al., 1997; Jones et al., 2000). Conversely, the higher

Table 3
Water strikes recorded during the drilling of the Merrisons Lane (ML) and Park Farm (PF) boreholes in February 2011. SCF-SG = Sheringham Cliffs Formation – sands + gravels; SCF-BGT = Sheringham Cliffs Formation – Bacton Green Till Member; BLF = Briton's Lane Formation; WCF = Wroxham Crag Formation; LF = Lowestoft Formation; HF = Happisburgh Formation.

Strike	Parameter	ML BH1	ML BH2	ML BH3	PF BH1	PF BH2	PF BH3	PF BH4
1	Depth (m)	5.1	4.5	4.8	4.8	5.1	4.8	4.7
	Formation	SCF-SG	SCF-BGT	SCF-SG	BLF	BLF	BLF	BLF
	Inflow rate	Slow	Very slow	Moderate	Very slow	Very slow	Slow	Slow
2	Depth (m)	16.3	14.7		11.6			
	Formation	WCF	LF		HF			
	Inflow rate	Fast	slow		Moderate			
3	Depth (m)	21.5			17.2			
	Formation	Chalk			Chalk			
	Inflow rate	–			Moderate			

storage coefficient of the sandy Briton's Lane, Sheringham Cliffs and Happisburgh Formations result in greater effective water storage and thereby lower sensitivity to antecedent conditions at these medium timescales. At hourly-to-daily timescales, however, groundwater levels at Park Farm respond much faster to precipitation events due to the higher permeability of the sands, thus resulting in greater high-frequency variability within the Park Farm record.

Water strike depths recorded during the drilling of the boreholes in February 2011 revealed the top of the saturated aquifer formations at this time (Table 3). At Merrisons Lane, water strikes were recorded at ~5 m depth in both the Sheringham Cliffs Formation glacial sands and Bacton Green Till Member, where inflow rates were slow–moderate and very slow, respectively. Deeper water strikes occurred at 14.7 m in the Lowestoft Formation (slow inflow rate), 16.3 m in the Wroxham Crag Formation (fast inflow rate) and at 21.5 m in the regional Chalk aquifer. At the Park Farm boreholes, water strikes were recorded at ~ 5 m in the Briton's Lane Formation (slow – very slow inflow rates), at 11.6 m in the Happisburgh Formation (moderate inflow rate) and at 17.2 m in the Chalk (moderate inflow rate).

3.4. Hyporheic zone

The physical properties of the hyporheic zone sediments recorded at the five piezometer locations are summarised in Table 4. All locations were in the western section of the Blackwater Drain associated with the lower permeability glacial deposits and the majority of sites at 0.5 and 1.0 m depth were comprised of either sandy clay loam or clay sediments. Bulk densities across the sites ranged from 0.19 to 2.36 g cm^{-3} and porosities from 2.6 to 34.8%, whilst hydraulic conductivities ranged from a low of 5.2×10^{-6} m s^{-1} to a high of 6.2×10^{-3} m s^{-1}, but there was no evidence of seasonality during the April 2016 to January 2017 monitoring period. Piezometer recharge rate also remained fairly consistent with depth across the 0.5–1.5 m profile, although mean conductivities were significantly higher at site 5 lower down the catchment, indicating higher rates of groundwater movement at this site. Piezometer recharge rates are usually related to the antecedent conditions within the catchment, thus explaining the greater than two orders of magnitude range of values recorded at individual sites and depths. Nevertheless, most of the values recorded here fall within the range expected (10^{-4}–10^{-5} m s^{-1}) for sediments with clay contents of 9–58%, based on a previous study by Shevnin et al. (2006) who modelled hydraulic conductivity using resistivity data for sediments with increasing clay content. Some of the lower hydraulic conductivities (i.e. 10^{-6} m s^{-1}) could possibly be caused by smearing of the piezometer tip during installation and may not be an accurate reflection of groundwater-surface water interactions.

3.5. Soil water

Soil moisture content recorded in the sandy loam soils and sandy deposits developed on the Briton's Lane Formation at site F display a pronounced seasonal cycle of spring/summer drying and autumn/winter wetting throughout the 90 cm depth profile (Fig. 9a). Mean soil moisture content for the entire monitoring period steadily increased with depth from 49.0% at 10 cm depth to 56.6% at 90 cm depth, with the shallower depths exhibiting greater seasonal variability. At 10 cm depth, mean monthly soil moisture contents ranged from a low of 42.9% in August when evapotranspiration rates are high, to a maximum of 54.3% in December following autumn rewetting. This compares with mean monthly soil moisture contents at 90 cm depth of 55.9% in August and 57.7% in December, reflecting reduced evapotranspiration losses during the summer at deeper depths.

During storm events, distinct differences arise in the rewetting profile of clay loam (Fig. 9b) and sandy loam (Fig. 9c) soils, which reflect the impact of soil structure upon subsurface flow paths. The example presented here for the 7–13th March 2013 following 53 mm of rainfall, reveals that on the freely draining, light, sandy loam soils in the eastern Blackwater Drain sub-catchment, rainwater readily infiltrates down through the top 90 cm, with soil moisture content increasing from 36.8 to 41.7% at 10 cm depth and from 43.5 to 49.5% at 90 cm depth. In contrast, on the heavier clay-loam soils in the western part of the catchment, infiltration is severely impeded below 20 cm depth by the clay-rich Bacton Green Till Member deposits, such that there is no discernible increase in soil moisture content below this depth. It is also noted that the top 20 cm in clay loam soil exhibits a substantially larger response (~23% increase in moisture content) to the rainfall event than the sandy loam soil (~5% increase) indicating an increased risk of soil saturation and surface runoff generation. Similarly, the moisture peak at 20 cm occurs ~10 h earlier on the sandy loam soil reflecting a faster infiltration rate and thus a reduced risk of initiating surface flows.

For the subsurface agricultural field drains (Fig. 10), soil water discharges into the Blackwater Drain varied depending upon season and antecedent moisture conditions. Most drains dried up completely between April and September as groundwater levels across the catchment fell below the depth of the drains; this depth being below ~41.5 m a.s.l. at the Merrisons Lane boreholes. The highest drain discharge (2.96 l s^{-1}) was recorded under clay soil in November 2015 following heavy rainfall (32 mm) over the preceding 7 days. Over the whole monitoring period, mean discharges were significantly ($p < 0.05$) higher under clay/clay loam soils (0.22 l s^{-1}; $\sigma = 0.33$ l s^{-1}) than sandy loam soils (0.07 l s^{-1}; $\sigma = 0.06$ l s^{-1}), revealing increased potential for the direct quickflow transport of pollutants into the river through this preferential pathway. The mean drain catchment area was also significantly ($p < 0.05$) higher under clay/clay loam soils (2.0 ha; $\sigma = 1.9$ ha)

Table 4
Physical properties of the hyporheic zone sediments recorded at the five piezometer locations. Hydraulic conductivity presented as the mean with the range in parentheses.

Site	Depth (m)	Porosity (%)	Bulk Density (g cm^{-3})	Sand (%)	Silt (%)	Clay (%)	Sediment Type	Hydraulic Conductivity (m s^{-1})
1	0.5	2.6	2.36	30	19	51	Clay	1.1×10^{-4} (8.6×10^{-6} – 4.2×10^{-4})
1	1.0	22.4	1.00	17	26	57	Clay	2.2×10^{-4} (8.1×10^{-5} – 6.9×10^{-4})
1	1.5	–	–	–	–	–	–	3.6×10^{-4} (2.0×10^{-5} – 9.5×10^{-4})
2	0.5	12.6	0.19	85	6	9	Loamy sand	2.0×10^{-4} (6.1×10^{-5} – 9.5×10^{-4})
2	1.0	17.5	1.20	36	21	43	Clay	8.7×10^{-5} (1.8×10^{-5} – 2.5×10^{-4})
2	1.5	–	–	–	–	–	–	7.3×10^{-4} (2.0×10^{-4} – 2.3×10^{-3})
3	0.5	17.8	1.10	61	13	26	Sandy clay loam	5.5×10^{-5} (3.0×10^{-5} – 8.0×10^{-5})
3	1.0	16.7	1.44	35	18	47	Clay	6.5×10^{-5} (1.9×10^{-5} – 2.4×10^{-4})
3	1.5	–	–	–	–	–	–	7.4×10^{-5} (2.4×10^{-5} – 1.9×10^{-4})
4	0.5	22.3	1.15	46	20	34	Sandy clay loam	3.9×10^{-5} (1.3×10^{-5} – 1.2×10^{-4})
4	1.0	19.9	0.94	62	16	22	Sandy clay loam	2.8×10^{-5} (2.0×10^{-5} – 9.5×10^{-5})
4	1.5	–	–	–	–	–	–	1.4×10^{-5} (5.2×10^{-6} – 2.7×10^{-5})
5	0.5	34.8	0.86	50	19	31	Sandy clay loam	1.7×10^{-3} (6.7×10^{-4} – 2.1×10^{-3})
5	1.0	24.6	1.19	26	16	58	Clay	1.7×10^{-3} (1.2×10^{-3} – 2.2×10^{-3})
5	1.5	–	–	–	–	–	–	4.0×10^{-3} (3.2×10^{-3} – 6.2×10^{-3})

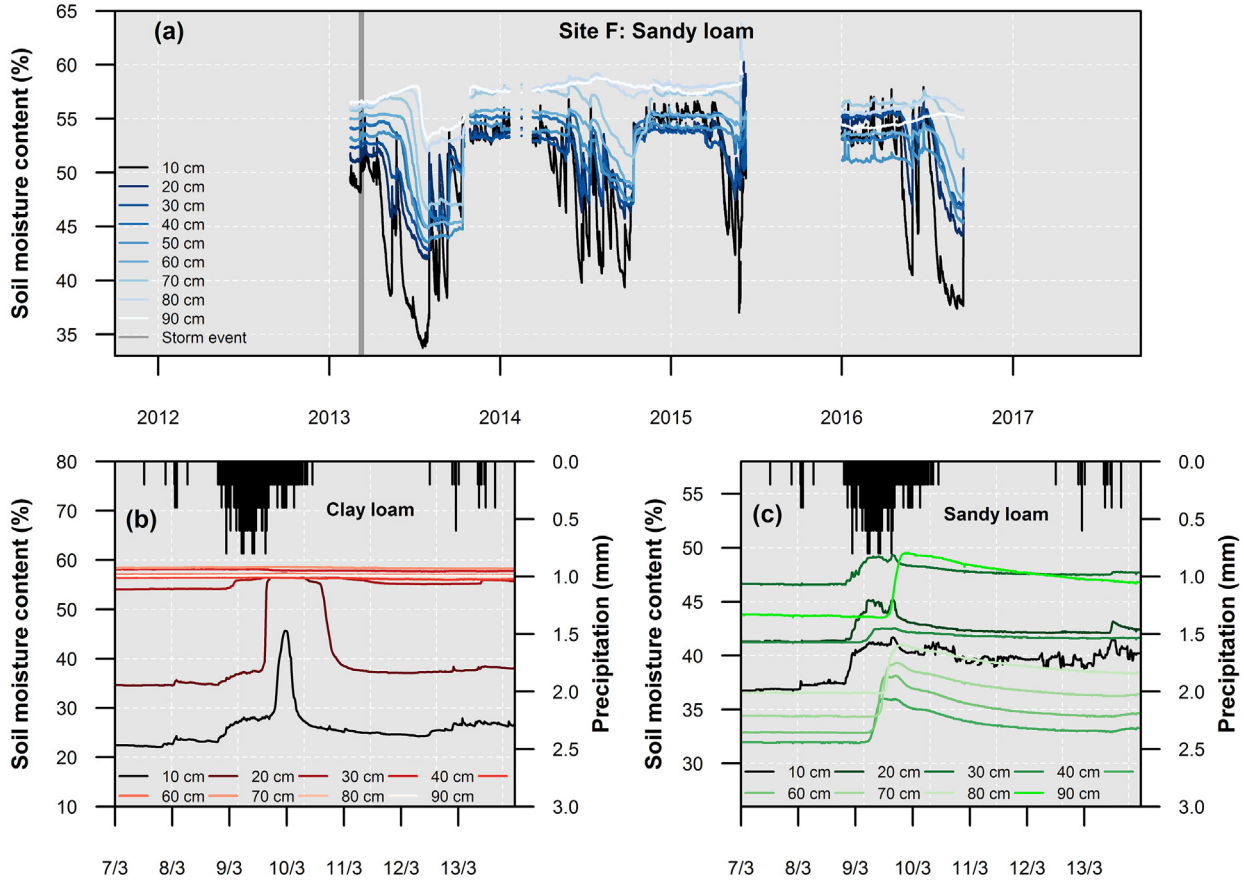

Fig. 9. Soil moisture content recorded at 10–90 cm depth in: (a) site F sandy loam soils between 2013 and 2016; and during a storm event (53 mm precipitation) in March 2013 on (b) clay loam soils in mini-catchment A and (c) sandy loam soils in mini-catchment D.

than sandy loam soils (0.4 ha; $\sigma = 0.4$ ha), which intuitively suggests that this difference was responsible for the greater discharge observed under heavier textured soils. However, drain discharge and drain catchment area were weakly and insignificantly correlated ($R^2 = 0.07$; $p = 0.40$) implying causality is unlikely. Instead, it is probable that the lower drain flows observed under sandy soils are a result of infiltrating precipitation bypassing the drain network as it percolates freely down to the shallow groundwater. Under clay soils, infiltrating precipitation is impeded from reaching the shallow groundwater table, meaning more water remains in the surface soils where it can enter into field drainage and be exported via quickflow into the river network bypassing the deeper geology (Deasy et al., 2009; King et al., 2015; Kronvang et al., 2007).

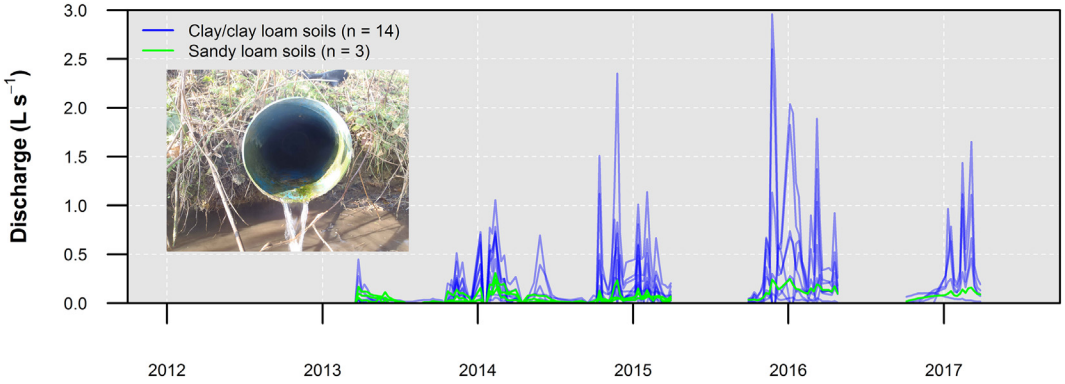

Fig. 10. Soil water discharge rates from subsurface agricultural field drains recorded under contrasting soil types during 2013–2017.

3.6. Storm event responses

Fluvial hydrographs displaying typical storm event responses at sites A, C and F are shown in Fig. 11 for example summer (June 2016) and winter (November 2012) events. During the summer storm event on the 23 June 2016, 29.6 mm of rainfall fell in just 4 h with a total of 48 mm of rainfall falling over the whole seven day period shown (23–29 June). In response, river discharge increased 30-fold at site A, 12-fold at site C and 10-fold at site F between pre-event conditions and peak flow conditions. The larger, flashier response at site A reflects the greater proportion of surface runoff in mini-catchment A (lower BFI) compared to mini-catchment C (higher BFI), where a more permeable superficial geology allows for greater infiltration and groundwater recharge. Furthermore, the time between precipitation onset and peak discharge was 6 h 45 min at site A, 3 h 15 min at site C and 5 h 15 min at site F. This slower response time in mini-catchment A reflects the lower permeability of the clay-rich soils and glacial deposits, which correspondingly slows the flow of event water (i.e. soil through-flow) into the river.

During the winter storm event in late-November 2012, three main bands of precipitation delivered a total of 48 mm of rainfall over 7 days (24–30 November) resulting in three distinct peaks in the hydrograph at sites A, F and, to a lesser extent, site C. As with the summer event, site A displayed the largest, flashy response with discharge increasing 5-fold between pre-event conditions and peak discharge of the first event, compared to 3-fold increases observed at sites C and F. Unlike the summer event, however, the response times between precipitation onset and peak discharge were very similar at sites A and C for the first (~18 h), second (~7h) and third (~12 h) winter events. This comparatively faster response time at site A, relative to site C, than observed during the summer event can be explained by the activation of the subsurface field drains in mini-catchment A, which by late-November are flowing continuously due to the rise in groundwater levels and so providing a preferential pathway for the transport of event water into the river.

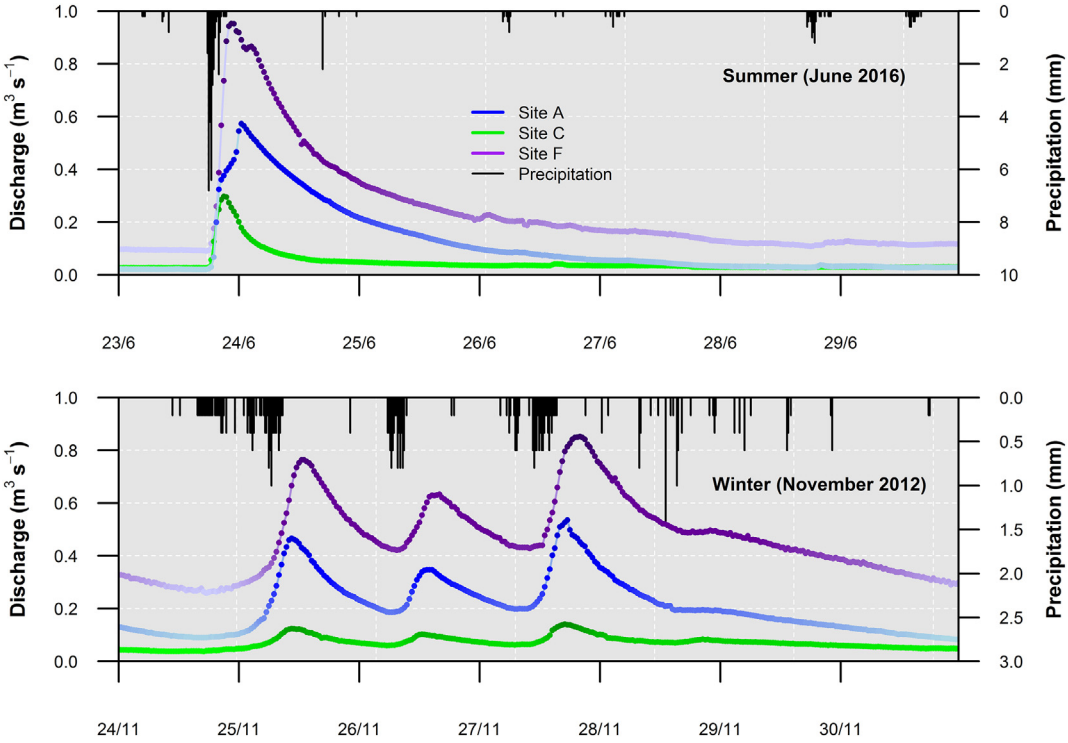

Fig. 11. Fluvial hydrographs displaying typical storm event responses during example summer (June 2016) and winter (November 2012) periods at sites A, C and F.

3.7. Catchment water balance

Annual evapotranspiration (E_T) estimates for mini-catchments A, C and F were derived using a simple catchment water balance approach (Table 5). The surface runoff (S_R) and groundwater discharge (G_R) components of total river flow (Q), calculated using hydrograph separation, were subtracted from annual precipitation totals to yield evapotranspiration estimates over the mini-catchment areas.

Mini-catchment A experienced the highest mean annual evapotranspiration rate (548 mm), accounting for ~ 80% of total precipitation and yielding a mean annual effective precipitation total of 139 mm. This compares with mini-catchment C which had a significantly ($p < 0.05$) lower mean annual evapotranspiration rate of 408 mm, accounting for 59% of total precipitation and yielding a mean annual effective precipitation total of 279 mm. This difference can be explained by the lower permeability of the argillaceous deposits underlying mini-catchment A, which reduce infiltration rates and leave more water available near the soil surface for evapotranspiration. In mini-catchment C, the high permeability sandy Briton's Lane Formation deposits readily allow infiltration down to the shallow groundwater, which then supplies greater groundwater discharge in support of river baseflow. A direct consequence of the lower effective precipitation totals in mini-catchment A is that this area is more susceptible to drought and increases the risk of the river in this part of the catchment drying up completely during the summer months. Evidence for this can be seen in Fig. 6, where the minimum summer flow recorded at site A (0.0004 m^3 s^{-1}) was an order of magnitude lower than observed at site C (0.0049 m^3 s^{-1}), despite the area of mini-catchment A being 54% larger than mini-catchment C.

Groundwater storage coefficients were also estimated using the borehole hydrograph method (Hiscock and Bense, 2014). This was achieved by dividing the annual groundwater discharge (G_R) found by stream hydrograph separation by the change in amplitude of groundwater (Δh) in the shallowest borehole (Table 5). This yielded mean groundwater storage coefficients of 0.027 for the Bacton Green Till Member and 0.216 for the Briton's Lane Formation, values comparable with those reported previously for Quaternary glaciogenic deposits (Morris and Johnson, 1967).

3.8. Conceptual models

Interpreting these high-resolution monitoring data, it is possible to construct conceptual models of hydrological processes across areas of contrasting hydrogeological conditions (e.g. Rozemeijer and Broers, 2007) within the Blackwater Drain sub-catchment (Figs. 12 and 13).

In the western section, the low permeability, argillaceous superficial deposits of the Sheringham Cliffs Formation Bacton Green Till Member and Lowestoft Formation restrict rainwater infiltration and inhibit recharge to the underlying confined Wroxham Crag and Cretaceous Chalk aquifers. This reduced downward movement of water leads to increased risk of soil saturation – as detected by soil moisture probe monitoring down to 90 cm depth – and consequent activation of surface runoff pathways during heavy precipitation events as infiltration capacity is exceeded – as determined by river discharge monitoring with pressure transducers. This produces a river with a comparatively low groundwater/surface water ratio (BFI = 0.50) – as determined by hydrograph separation – where river levels vary widely from low in summer to high in winter. Agricultural field drains artificially lower the water table in the Bacton Green Till Member during the winter months to prevent waterlogging in the root zone, providing a quickflow pathway for the export of water into the surface watercourse – as determined by measuring field drain discharges and borehole monitoring of groundwater levels. The Holocene alluvium and river terrace deposits are usually in hydraulic continuity with the associated river – as determined by piezometer monitoring of hydraulic conductivity within the hyporheic zone down to 1.5 m depth. Within the Bacton Green Till, frequent bands of oxidised iron reveal evidence of water flow through lateral and vertical fissures, as inferred by Hiscock and Tabatabai Najafi (2011), within these otherwise low permeability deposits (Table S1). At greater depth the glaciolacustrine and glaciofluvial sands of the Sheringham Cliffs Formation provide a zone of increased permeability and can become saturated forming a shallow aquifer, as determined through borehole monitoring of groundwater levels and water strike depths.

In contrast, in the eastern section the high permeability sands of the Briton's Lane Formation allow for rapid infiltration of precipitation (derived from 15-min resolution rain gauge measurements)

Table 5
Annual catchment water balance for mini-catchments A, C and F in the Blackwater Drain sub-catchment. P = precipitation; S_R = surface water runoff; G_R = groundwater discharge; E_T = evapotranspiration; Δh = amplitude of groundwater level change; S = groundwater storage coefficient.

Site	Year	P (mm)	Stream hydrograph separation			Borehole hydrograph storage estimation	
			S_R (mm)	G_R (mm)	E_T (mm)	Δh BH4 (mm)	S
A	2011/12	694	70*	60*	564*	2530	–
	2012/13	638	95	85	458	2705*	0.031
	2013/14	724	55	74	595	2290	0.032
	2014/15	715	70	88	557	3075	0.029
	2015/16	724	70	63	591	2156	0.032
	2016/17	632	46	49	537	3256	0.015
C	2011/12	694	32*	92*	570*	879	–
	2012/13	638	84	237	317	1091	0.217
	2013/14	724	56	210	458	888	0.236
	2014/15	715	40	171	504	906	0.189
	2015/16	724	62	216	446	1236	0.175
	2016/17	632	56	262	314	989	0.265
F	2011/12	694	38	71	585	1705	0.042
	2012/13	638	72	128	438	1898*	0.067
	2013/14	724	52	101	571	1589	0.064
	2014/15	715	36	79	600	1991	0.040
	2015/16	724	70	125	529	1696	0.074
	2016/17	632	39	90	503	2123	0.042

* Calculation affected by missing data.

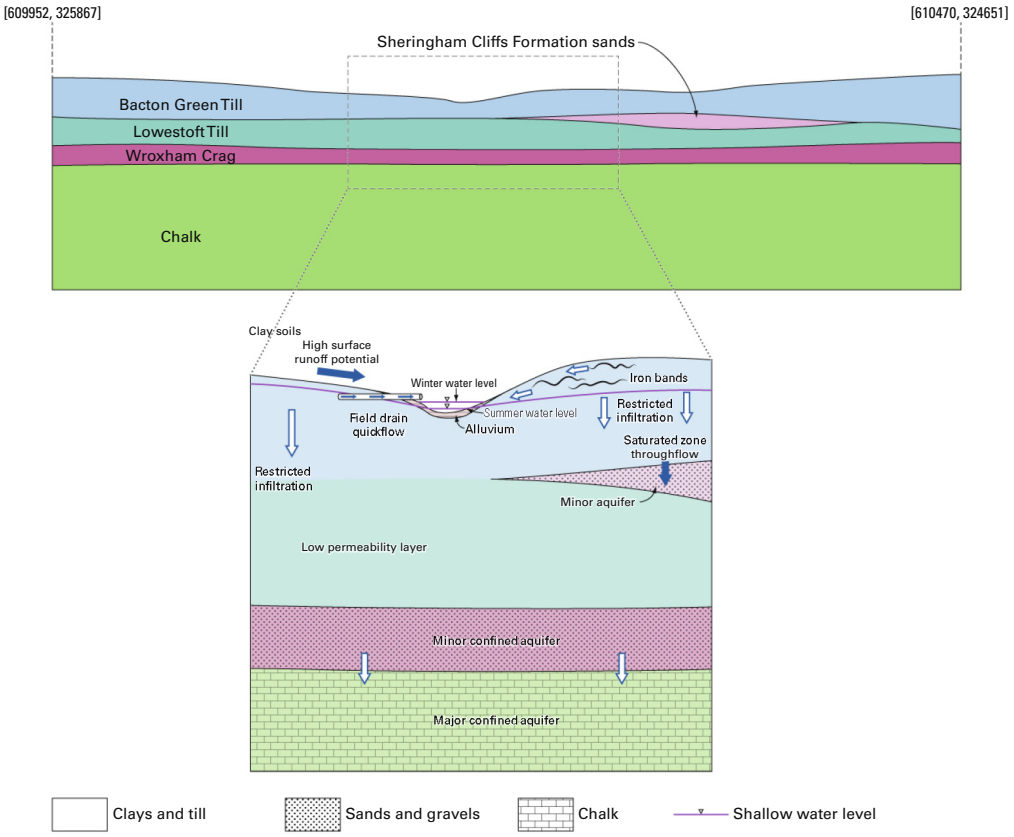

Fig. 12a. Simplified 2-D conceptual model of hydrogeological processes in the western section of the Blackwater Drain sub-catchment. Blue arrows represent the dominant water flow paths; white arrows the minor flow pathways. BGS © UKRI 2018. (For interpretation of the references to colour in this figure legend, the reader is referred to the web version of this article.)

away from the soil surface. This reduces the potential for soil saturation – as determined from soil moisture probes – and the initiation of surface runoff as determined by monitoring of river discharge storm event response. This negates the requirement for artificial field drainage – reducing the availability of artificial quickflow pathways in this part of the catchment – and produces a river with a comparatively high groundwater/surface water ratio (BFI = 0.78) and stable year round water levels – as determined by pressure transducer river stage monitoring. Saturation of the Briton's Lane sands forms a shallow aquifer that rests above lower permeability deposits of the Sheringham Cliffs Formation glaciolacustrine clay – as determined from borehole groundwater level monitoring. As presented by Hiscock et al. (2011), interdigitation of the glacial tills with glaciofluvial and glaciolacustrine sands provides a zone of saturated throughflow that sits above the confining layer of the low-permeability Lowestoft Formation. The Lowestoft Till Member inhibits recharge to the underlying Happisburgh Formation and Cretaceous Chalk aquifers, which are largely in hydraulic continuity.

In both the eastern and western sections of the Blackwater Drain catchment, the channel morphology (e.g. sinuosity, gradient, connectivity, pools, riffles) and within-channel processes (e.g. density of emergent and submergent macrophyte growth), will impact upon the hydrological functioning of these river systems (e.g. storm event response times), although these are not currently monitored as part of the Wensum DTC research project.

3.9. Implications for agricultural management practices

The hydrogeological characteristics of this region have a number of important implications for land management practices, particularly in relation to the implementation of on-farm mitigation measures to reduce agricultural water pollution. Some example measures are considered below:

(i) **Winter cover crops** – evidence from the high-resolution soil moisture probe data demonstrates that the sandy soils and sandy deposits of the Briton's Lane Formation in the east of the catchment are highly vulnerable to nutrient (principally nitrate) and pesticide leaching into the shallow groundwater. The use of cover crops to provide overwinter soil cover has been shown to significantly reduce nutrient leaching losses by taking up both excess fertiliser and excess soil moisture (Dabney et al., 2001; Stevens and Quinton, 2009) and would therefore be recommended as an on-farm pollution mitigation measure in this area. The soil moisture probe data also reveal that the western section of the catchment under clay-rich soils suffers from restricted infiltration below 20 cm depth and is therefore at increased risk of soil saturation and the generation of erosive surface runoff. The use of deep-rooting cover crop varieties, such as oilseed radish (Cooper et al., 2017), would be recommended for these conditions as they can help to break up compacted soil and create larger pores and fissures which increase permeability and infiltration rates and help to transport water away from the soil surface.

(ii) **Reduced tillage** – the short response times observed in river flow, soil moisture content and groundwater levels to precipitation events in the sandy mini-catchment C reflect the limited capability of these soils and superficial deposits to retain water. This rapid transport of event water into surface

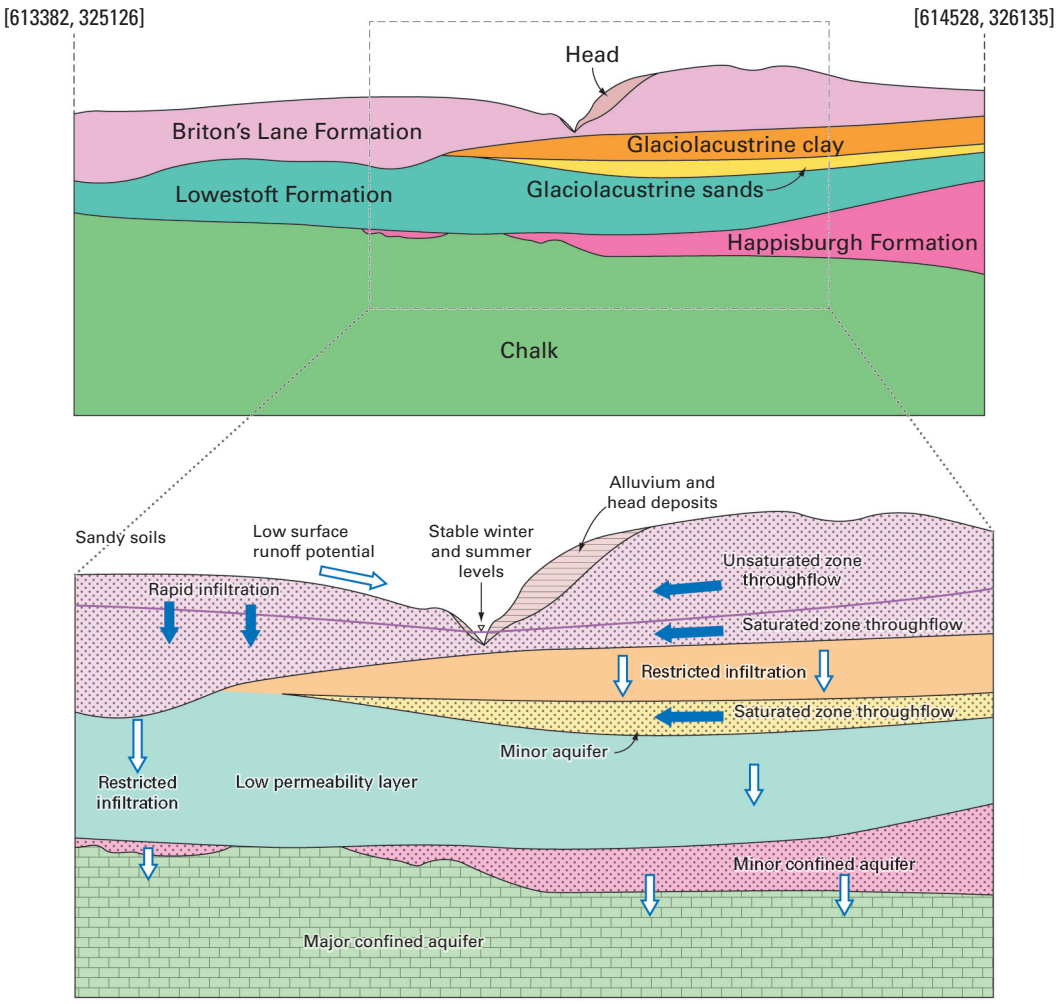

Fig. 12b. Simplified 2-D conceptual model of hydrogeological processes in the eastern section of the Blackwater Drain sub-catchment. Blue arrows represent the dominant water flow paths; white arrows the minor flow pathways. BGS © UKRI 2018. (For interpretation of the references to colour in this figure legend, the reader is referred to the web version of this article.)

watercourses provides reduced opportunities for pollutant attenuation and thereby elevates water pollution risk. Reduced tillage practiced over several years has been shown to increase soil organic carbon contents, which in turn can improve both the structural stability and water holding capacity of the soil, thus helping to slow storm event response times in sandy catchments (Holland, 2004; Soane et al., 2012).

(iii) **Application timing** – agricultural field drains have been shown to act as important preferential pathways for the export of soil water into the river network under clay-rich soils. This pathway is most active between October and March when drain flows are high and thus application of agrochemicals during this period will carry increased water pollution risk. Where possible, applications outside of this period would be recommended to reduce pollutant mobility within the environment. However, it should also be noted that river discharge was very low during the summer months where argillaceous deposits predominated and this carries with it the risk of concentrating riverine pollutants during the most ecologically sensitive season if measures are not put in place to reduce agrochemical input at this time. Whilst it will not always be agronomically feasible to cease agrochemical applications, the high-temporal resolution water quality monitoring presented here can at least assist in demonstrating the scale and timing of water and nutrient losses out of agricultural areas and make farmers aware of the need to consider best practices for how and when to make fertiliser and pesticide applications.

The interpretations made here are applicable not just to southeast England, but also more widely across northwest Europe (Eissmann, 2002; Kasse, 2002) and North America (Fortin et al., 1991; Gleeson et al., 2014; Ross et al., 2004), where similar Quaternary glaciogenic geology can be found. In Denmark, for example, Tertiary and Cretaceous Limestone in the east of the country is overlain by complex sequences of sandy/clayey tills and sandy/gravelly glacial outwash deposits, resulting in a very similar hydrogeological setting to the Blackwater Drain sub-catchment (Jørgensen and Stockmarr, 2008). Denmark's rivers are also largely groundwater fed, as in southeast England, and the landscape is similarly dominated by agriculture (62%; European Environment Agency, 2018) and thus experiences many of the same issues with diffuse water pollution raised here which necessitate the adoption of on-farm mitigation measures (Jørgensen and Stockmarr, 2008; Thomsen et al., 2004).

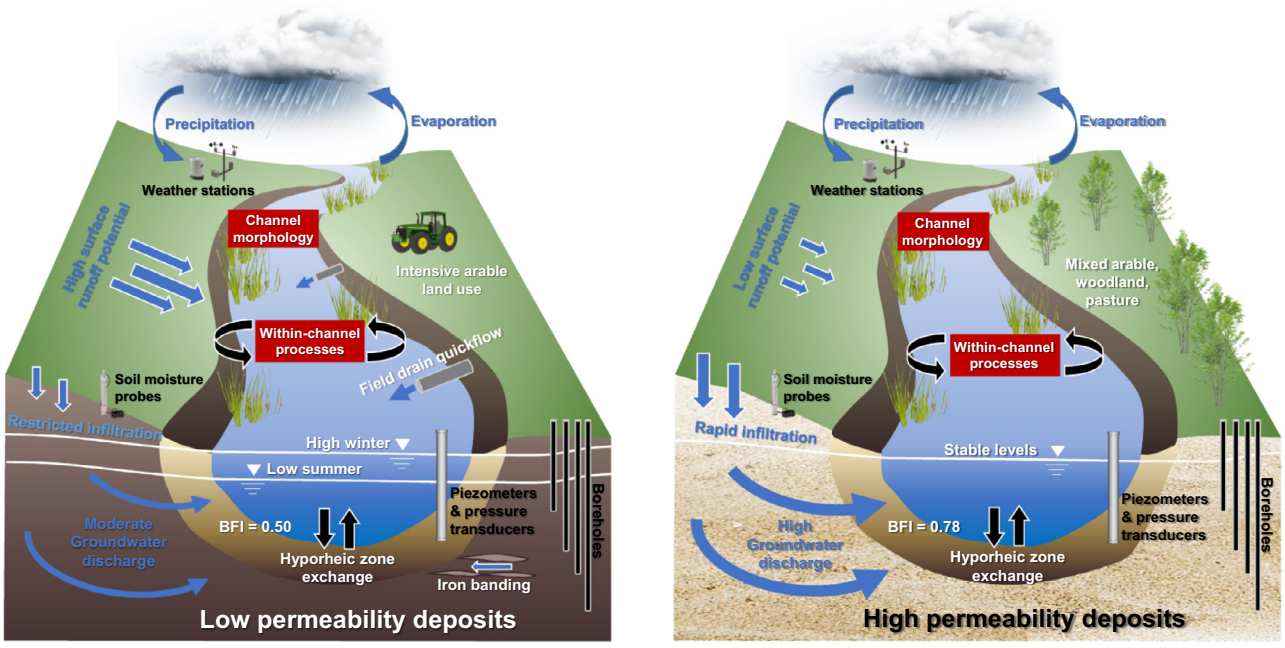

Fig. 13. 3-D conceptual models of hydrogeological processes in the western (left) and eastern (right) sections of the Blackwater Drain sub-catchment. Blue arrows denote the major flow paths monitored as part of the Wensum DTC platform; black labels highlight the Wensum DTC monitoring infrastructure; red boxes denote processes not currently monitored, but which likely impact upon fluvial dynamics. (For interpretation of the references to colour in this figure legend, the reader is referred to the web version of this article.)

4. Conclusions

This study has demonstrated how automated telemetered sensor technology can be applied to generate high-temporal resolution empirical datasets of hydrological and meteorological parameters from which conceptual models of catchment hydrogeological processes can be developed. The importance of improving our understanding of hydrogeological processes cannot be emphasised strongly enough, as ultimately it is the catchment hydrogeology which determines pollutant mobility within the environment as well as within-river pollutant behaviour. Gathering of such detailed datasets enables a more robust assessment to be made of the likely effectiveness of deploying on-farm mitigation measures to reduce agricultural water pollution, and this enhanced knowledge can help underpin the development of more effective, integrated and holistic river basin management plans incorporating groundwater – surface water interactions.

Conflict of interest

The authors declare no conflict of interest.

Acknowledgements

The River Wensum Demonstration Test Catchment project is funded by the Department for Environment, Food and Rural Affairs (Defra) under projects WQ0212 and LM0304. NLG was financially supported by a NERC EnvEast Doctoral Training Programme grant. ZQH acknowledges support from the Iraqi Kurdistan Regional Government. We are grateful to Salle Farms Co. and the Heydon Estate for hosting monitoring equipment and granting site access. We thank Simon Ellis, Jenny Stevenson and John Brindle for fieldwork support, and Helen Burke and Ricky Terrington for compiling the 3D geological model. We thank the anonymous reviewer for their constructive comments on this paper.

Appendix A. Supplementary data

Supplementary data to this article can be found online at https://doi.org/10.1016/j.hydroa.2018.100007.

References

Allen, D.J. et al., 1997. The physical properties of major aquifers in England and Wales. Brit. Geol. Surv. Tech. Rep. WD/97/34.
Allen, D.J. et al., 2014. Groundwater conceptual models: implications for evaluating diffuse pollution mitigation measures. Q. J. Eng. Geol. Hydrogeol. 47 (1), 65–80. https://doi.org/10.1144/qjegh2013-043.
Biddulph, M., Collins, A.L., Foster, I.D.L., Holmes, N., 2017. The scale problem in tackling diffuse water pollution from agriculture: insights from the Avon Demonstration Test Catchment programme in England. River Res. Appl. 33 (10), 1527–1538. https://doi.org/10.1002/rra.3222.
Bowes, M.J. et al., 2015. Characterising phosphorus and nitrate inputs to a rural river using high-frequency concentration-flow relationships. Sci. Total Environ. 511, 608–620. https://doi.org/10.1016/j.scitotenv.2014.12.086.
Brantley, S.L., McDowell, W.H., Dietrich, W.E., White, T.S., Kumar, P., Anderson, S.P., Chorover, J., Ann Lohse, K., Bales, R.C., Richter, D.D., Grant, G., Gaillardet, J., 2017. Designing a network of critical zone observatories to explore the living skin of the terrestrial Earth. Earth Surf. Dynam. 5, 841–860. https://doi.org/10.5194/esurf-5-841-2017.
Brunner, P., Cook, P.G., Simmons, C.T., 2011. Disconnected surface water and groundwater: from theory to practice. Groundwater 49, 460–467. https://doi.org/10.1111/j.1745-6584.2010.00752.x.
CEH, 2017. National River Flow Archive. https://nrfa.ceh.ac.uk/data/search. 17/07/2017.
Chapman, T., 1999. A comparison of algorithms for stream flow recession and baseflow separation. Hydrol. Process. 13, 701–714.
Collins, A.L. et al., 2013. Contemporary fine-grained bed sediment sources across the River Wensum Demonstration Test Catchment, UK. Hydrol. Processes 27 (6), 857–884. https://doi.org/10.1002/hyp.9654.
Cook, P.G., 2015. Quantifying river gain and loss at regional scales. J. Hydrol. 531, 749–758. https://doi.org/10.1016/j.jhydrol.2015.10.052.
Cooper, R.J., Battams, Z.M., Pearl, S.H., Hiscock, K.M., 2019. Mitigating river sediment enrichment through the construction of roadside wetlands. J. Environ. Manag., 231, 146–154.
Cooper, R.J. et al., 2016a. Assessing the effectiveness of a three-stage on-farm biobed in treating pesticide contaminated wastewater. J. Environ. Manage. 181, 874–882. https://doi.org/10.1016/j.jenvman.2016.06.047.

Cooper, R.J. et al., 2017. Assessing the farm-scale impacts of cover crops and non-inversion tillage regimes on nutrient losses from an arable catchment. Agric. Ecosyst. Environ. 237, 181–193. https://doi.org/10.1016/j.agee.2016.12.034.
Cooper, R.J., Krueger, T., Hiscock, K.M., Rawlins, B.G., 2015a. High-temporal resolution fluvial sediment source fingerprinting with uncertainty: a Bayesian approach. Earth Surf. Proc. Land. 40 (1), 78–92. https://doi.org/10.1002/esp.3621.
Cooper, R.J., Outram, F.N., Hiscock, K.M., 2016b. Diel turbidity cycles in a headwater stream: evidence of nocturnal bioturbation. J. Soils Sediments 16, 10.
Cooper, R.J. et al., 2015b. Apportioning sources of organic matter in streambed sediments: an integrated molecular and compound-specific stable isotope approach. Sci. Total Environ. 520, 187–197. https://doi.org/10.1016/j.scitotenv.2015.03.058.
Cooper, R.J. et al., 2015c. Contrasting controls on the phosphorus concentration of suspended particulate matter under baseflow and storm event conditions in agricultural headwater streams. Sci. Total Environ. 533, 49–59. https://doi.org/10.1016/j.scitotenv.2015.06.113.
Covino, T., 2017. Hydrologic connectivity as a framework for understanding biogeochemical flux through watersheds and along fluvial networks. Geomorphology 227, 133–144. https://doi.org/10.1016/j.geomorph.2016.09.030.
Dabney, S.M., Delgado, J.A., Reeves, D.W., 2001. Using winter cover crops to improve soil and water quality. Commun. Soil Sci. Plant Anal. 32 (7–8), 1221–1250. https://doi.org/10.1081/css-100104110.
Deasy, C., Brazier, R.E., Heathwaite, A.L., Hodgkinson, R., 2009. Pathways of runoff and sediment transfer in small agricultural catchments. Hydrol. Process. 23 (9), 1349–1358. https://doi.org/10.1002/hyp.7257.
Dupas, R., Gascuel-Odoux, C., Gilliet, N., Grimaldi, C., Gruau, G., 2015. Distinct export dynamics for dissolved and particulate phosphorus reveal independent transport mechanisms in an arable headwater catchment. Hydrol. Process. 29 (14), 3162–3178. https://doi.org/10.1002/hyp.10432.
Dupas, R., Jomaa, S., Musolff, A., Borchardt, D., Rode, M., 2016. Disentangling the influence of hydroclimatic patterns and agricultural management on river nitrate dynamics from sub-hourly to decadal time scales. Sci. Total Environ. 571, 791–800. https://doi.org/10.1016/j.scitotenv.2016.07.053.
Eissmann, L., 2002. Quaternary geology of eastern Germany (Saxony, Saxon-Anhalt, South Brandenburg, Thuringia), type area of the Elsterian and Saalian stages in Europe. Quat. Sci. Rev. 21, 72.
European Environment Agency, 2018. Land use – state and impacts (Denmark). https://www.eea.europa.eu/soer/countries/dk/land-use-state-and-impacts-denmark. 16/04/2018.
Färe, R., Grosskopf, S., Weber, W.L., 2006. Shadow prices and pollution costs in U.S. agriculture. Ecol. Econ. 56 (1), 89–103. https://doi.org/10.1016/j.ecolecon.2004.12.022.
Fortin, G., van der Kamp, G., Cherry, J.A., 1991. Hydrogeology and hydrochemistry of an aquifer-aquitard system within glacial deposits, Saskatchewan, Canada. J. Hydrol. 126, 28.
Garnier, J., Billen, G., Hannon, E., Fonbonne, S., Videnina, Y., Soulie, M., 2002. Modelling the transfer and retention of nutrients in the drainage network of the Danube River. Estuar. Coast. Shelf Sci. 54, 258–308. https://doi.org/10.1006/ecss.2000.0648.
Garnier, J., Billen, G., 2016. Ecological processes and nutrient transfers from land to sea: a 25-year perspective on research and management of the Seine River system. In: Glibert, P., Kana, T. (Eds.), Aquatic Microbial Ecology and Biogeochemistry: A Dual Perspective. Springer, Cham, pp. 185–197.
Gleeson, T., Moosdorf, N., Hartmann, J., Van Beek, L.P.H., 2014. A glimpse beneath earth's surface: GLobal HYdrogeology MaPS (GLHYMPS) of permeability and porosity. Geophys. Res. Lett. 41, 8. https://doi.org/10.1002/2014GL059856.
Gomez-Velez, J.D., Harvey, J.W., 2014. A hydrogeomorphic river network model predicts where and why hyporheic exchange is important in large basins. Geophys. Res. Lett. 41, 6403–6412. https://doi.org/10.1002/2014GL061099.
Grieve, N., Clarke, S., Caswell, B., 2002. Macrophyte survey of the River Wensum SAC. Centre for Aquatic Plant Management, Natural England.
Halliday, S.J., Wade, A.J., Skeffington, R.A., Neal, C., Reynolds, B., Rowland, P., Neal, M., Norris, D., 2012. An analysis of long-term trends, seasonality and short-term dynamics in water quality from Plynlimon, Wales. Sci. Total Environ. 434, 186–200. https://doi.org/10.1016/j.scitotenv.2011.10.052.
Halliday, S.J., Skeffington, R.A., Bowes, M.J., Gozzard, E., Newman, J.R., Loewenthal, M., Palmer-Felgate, E.J., Jarvie, H.P., Wade, A.J., 2014. The water quality of the River Enborne, UK: observations from high-frequency monitoring in a rural, lowland river system. Water 6, 150–180. https://doi.org/10.3390/w6010150.
Harvey, J., Gooseff, M., 2015. River corridor science: hydrologic exchange and ecological consequences from bedforms to basins. Water. Resour. Res. 51, 6893–6922. https://doi.org/10.1002/2015WR017617.
Hering, D. et al., 2010. The European Water Framework Directive at the age of 10: a critical review of the achievements with recommendations for the future. Sci. Total. Environ. 408 (19), 4007–4019. https://doi.org/10.1016/j.scitotenv.2010.05.031.
Hilton, J., O'Hare, M., Bowes, M.J., Jones, J.I., 2006. How green is my river? a new paradigm of eutrophication in rivers. Sci. Total Environ. 365 (1–3), 66–83. https://doi.org/10.1016/j.scitotenv.2006.02.055.
Hiscock, K.M., Bense, V.F., 2014. Hydrogeology: principles and practice. Wiley Blackwell 517, pp.
Hiscock, K.M., Dennis, P.F., Saynor, P.R., Thomas, M.O., 1996. Hydrochemical and stable isotope evidence for the extent and nature of the effective Chalk aquifer of north Norfolk, UK. J. Hydrol. 180, 29.
Hiscock, K.M., George, M.A., Dennis, P.F., 2011. Stable isotope evidence for the hydrogeological characteristics of clay-rich till in northern East Anglia. Q. J. Eng. Geol. Hydrogeol. 44 (2), 173–189. https://doi.org/10.1144/1470-9236/10-006.
Hiscock, K.M., Lister, D.H., Boar, R.R., Green, F.M., 2001. An integrated assessment of long-term changes in the hydrology of three lowland rivers in eastern England. J. Environ. Manage. 61 (3), 195–214. https://doi.org/10.1006/jema.2000.0405.
Hiscock, K.M., Tabatabai Najafi, M., 2011. Aquitard characteristics of clay-rich till deposits in East Anglia, Eastern England. J. Hydrol. 405 (3–4), 288–306. https://doi.org/10.1016/j.jhydrol.2011.05.025.
Holland, J.M., 2004. The environmental consequences of adopting conservation tillage in Europe: reviewing the evidence. Agric. Ecosyst. Environ. 103 (1), 1–25. https://doi.org/10.1016/j.agee.2003.12.018.
Jones, H.K. et al., 2000. The physical properties of minor aquifers in England and Wales. Brit. Geol. Surv. Tech. Rep. WD/00/4.
Jørgensen, L.F., Stockmarr, J., 2008. Groundwater monitoring in Denmark: characteristics, perspectives and comparison with other countries. Hydrogeol. J. 17 (4), 827–842. https://doi.org/10.1007/s10040-008-0398-7.
Kasse, C., 2002. Sandy aeolian deposits and environments and their relation to climate during the last glacial maximum and late glacial in northwest and central Europe. Prog. Phys. Geogr. 26 (4), 26.
Kim, H., Dietrich, W.E., Thurnhoffer, B.M., Bishop, J.K.B., Fung, I.Y., 2017. Controls on solute concentration-discharge relationships revealed by simultaneous hydrochemistry observations of hillslope runoff and stream flow: the importance of critical zone structure. Water Resour. Res. 53, 1424–1443. https://doi.org/10.1002/2016WR019722.
King, K.W. et al., 2015. Phosphorus transport in agricultural subsurface drainage: a review. J Environ Qual 44 (2), 467–485. https://doi.org/10.2134/jeq2014.04.0163.
Kronvang, B., Vagstad, N., Behrendt, H., Bogestrand, J., Larsen, S.E., 2007. Phosphorus losses at the catchment scale within Europe: an overview. Soil Use Manag. 23, 13.
Lewis, M.A., 2014. Borehole drilling and sampling in the Wensum Demonstration Test Catchment. British Geological Survey Commissioned Report CR/11/162: 52.
Lloyd, C.E., Freer, J.E., Johnes, P.J., Collins, A.L., 2016a. Using hysteresis analysis of high-resolution water quality monitoring data, including uncertainty, to infer controls on nutrient and sediment transfer in catchments. Sci. Total Environ. 543 (Pt A), 388–404. https://doi.org/10.1016/j.scitotenv.2015.11.028.
Lloyd, C.E.M., Freer, J.E., Johnes, P.J., Coxon, G., Collins, A.L., 2016b. Discharge and nutrient uncertainty: implications for nutrient flux estimation in small streams. Hydrol. Process. 30 (1), 135–152. https://doi.org/10.1002/hyp.10574.
McGonigle, D.F. et al., 2014. Developing Demonstration Test Catchments as a platform for transdisciplinary land management research in England and Wales. Environ. Sci. Process Impacts 16 (7), 1618–1628. https://doi.org/10.1039/c3em00658a.
Met Office, 2017. UK Climate Averages. http://www.metoffice.gov.uk/public/weather/climate/?tab=climateStations. 17/07/2017.
Morris, D.A., Johnson, A.I., 1967. Summary of hydrologic and physical properties of rock and soil materials, as analyzed by the hydrologic laboratory of the U.S. Geological Survey. United States Geological Survey, Washington D.C.
Némery, J., Garnier, J., 2016. The fate of phosphorus. Nat. Geosci. 9 (5), 343–344. https://doi.org/10.1038/ngeo2702.
Newcomer, M.E., Hubbard, S.S., Fleckenstein, J.H., Maier, U., Schmidt, C., Thullner, M., Ulrich, C., Flipo, N., Rubin, Y., 2018. Influence of hydrological perturbations and riverbed sediment characteristics on hyporheic zone respiration of CO_2 and N_2. J. Geophys. Res. Biogeosci. 123, 902–922. https://doi.org/10.1002/2017JG004090.
Nolan, B.T., Hitt, K.J., 2006. Vulnerability of shallow groundwater and drinking-water wells to nitrate in the United States. Environ. Sci. Technol. 40, 7834–7840. https://doi.org/10.1021/es060911u.
Ockenden, M.C. et al., 2017. Prediction of storm transfers and annual loads with data-based mechanistic models using high-frequency data. Hydrol. Earth Syst. Sci. 21 (12), 6425–6444. https://doi.org/10.5194/hess-21-6425-2017.
Outram, F.N., Cooper, R.J., Sunnenberg, G., Hiscock, K.M., Lovett, A.A., 2016. Antecedent conditions, hydrological connectivity and anthropogenic inputs: factors affecting nitrate and phosphorus transfers to agricultural headwater streams. Sci. Total Environ. 545–546, 184–199. https://doi.org/10.1016/j.scitotenv.2015.12.025.
Outram, F.N. et al., 2014. High-frequency monitoring of nitrogen and phosphorus response in three rural catchments to the end of the 2011–2012 drought in England. Hydrol. Earth Syst. Sci. 18 (9), 3429–3448. https://doi.org/10.5194/hess-18-3429-2014.
Perks, M.T. et al., 2015. Dominant mechanisms for the delivery of fine sediment and phosphorus to fluvial networks draining grassland dominated headwater catchments. Sci. Total Environ. 523, 178–190. https://doi.org/10.1016/j.scitotenv.2015.03.008.
Popp, J., Pető, K., Nagy, J., 2012. Pesticide productivity and food security. A review. Agron. Sustainable Dev. 33 (1), 243–255. https://doi.org/10.1007/s13593-012-0105-x.
Pretty, J.N. et al., 2003. Environmental costs of freshwater eutrophication in England and Wales. Environ. Sci. Technol. 37 (2), 8. https://doi.org/10.1021/es020793k.
Quinton, J.N., Govers, G., Van Oost, K., Bardgett, R.D., 2010. The impact of agricultural soil erosion on biogeochemical cycling. Nat. Geosci. 3 (5), 311–314. https://doi.org/10.1038/ngeo838.
Rode, M. et al., 2015. The importance of hyporheic zone processes on ecological functioning and solute transport of streams and rivers. In: Chicharo, L., Müller,

F., Fohrer, N. (Eds.), Ecosystem Services and River Basin Ecohydrology. Springer, Netherlands, Dordrecht, pp. 57–82.
Rode, M. et al., 2016. Sensors in the stream: the high-frequency wave of the present. Environ. Sci. Technol. 50 (19), 10297–10307. https://doi.org/10.1021/acs.est.6b02155.
Ross, M., Parent, M., Lefebvre, R., 2004. 3D geologic framework models for regional hydrogeology and land-use management: a case study from a Quaternary basin of southwestern Quebec, Canada. Hydrogeol. J. 13 (5–6), 690–707. https://doi.org/10.1007/s10040-004-0365-x.
Rozemeijer, J.C., Broers, H.P., 2007. The groundwater contribution to surface water contamination in a region with intensive agricultural land use (Noord-Brabant, The Netherlands). Environ. Pollut. 148 (3), 695–706. https://doi.org/10.1016/j.envpol.2007.01.028.
Sear, D.A., Newson, M., Old, J.C., Hill, C., 2006. In: Nature, E. (Ed.), Geomorphological appraisal of the River Wensum Special Area of Conservation. Northminster House, Peterborough, p. 47.
Shevnin, V., Delgado Rodrìguez, O., Mousatov, A., Hernández, D.F., Martìnez, H.Z., Ryjov, A., 2006. Estimation of soil petrophysical parameters from resistivity data: application to oil-contaminated site characterization. Geofis. Int. 45, 179–193.
Skinner, J.A., Lewis, K.A., Bardon, K.S., Tucker, P., Catt, J.A., Chambers, B.J., 1997. An overview of the environmental impact of agriculture in the U.K. J. Environ. Manage. 50, 111–128.
Smith, V.H., Tilman, G.D., Nekola, J.C., 1999. Eutrophication: impacts of excess nutrient inputs on freshwater, marine, and terrestrial ecosystems. Environ. Pollut. 100, 179–196.
Soane, B.D. et al., 2012. No-till in northern, western and south-western Europe: a review of problems and opportunities for crop production and the environment. Soil Tillage Res. 118, 66–87. https://doi.org/10.1016/j.still.2011.10.015.
Stevens, C.J., Quinton, J.N., 2009. Diffuse pollution swapping in arable agricultural systems. Crit. Rev. Environ. Sci. Technol. 39 (6), 478–520. https://doi.org/10.1080/10643380801910017.
Thomsen, R., Sondergaard, V.H., Sorensen, K.I., 2004. Hydrogeological mapping as a basis for establishing site-specific groundwater protection zones in Denmark. Hydrogeol. J. 12 (5), 550–562. https://doi.org/10.1007/s10040-004-0345-1.
Toynton, R., 1983. The relation between fracture patterns and hydraulic anisotropy in the Norfolk Chalk, England. Q. J. Eng. Geol. Hydrogeol. 16, 17.
Voulvoulis, N., Arpon, K.D., Giakoumis, T., 2017. The EU Water Framework Directive: from great expectations to problems with implementation. Sci. Total Environ. 575, 358–366. https://doi.org/10.1016/j.scitotenv.2016.09.228.
Vuorenmaa, J., Augustaitis, A., Beudert, B., Bochenek, W., Clarke, N., de Wit, H.A., Dirnböck, T., Frey, J., Hakola, H., Kleemola, S., Kobler, J., Krám, P., Lindroos, A.-J., Lundin, L., Löfgren, S., Marchetto, A., Pecka, T., Schulte-Bisping, H., Skotak, K., Srybny, A., Szpikowski, J., Ukonmaanaho, L., Váňa, M., Åkerblom, S., Forsius, M., 2018. Long-term changes (1990–2015) in the atmospheric deposition and runoff water chemistry of sulphate, inorganic nitrogen and acidity for forested catchments in Europe in relation to changes in emissions and hydrometerological conditions. Sci. Total Environ. 625, 1129–1145. https://doi.org/10.1016/j.scitotenv.2017.12.245.
Withers, P.J., Jarvie, H.P., 2008. Delivery and cycling of phosphorus in rivers: a review. Sci. Total Environ. 400 (1–3), 379–395. https://doi.org/10.1016/j.scitotenv.2008.08.002.